Monocyte-derived extracellular vesicles stimulate cytokinesecretion and gene expression of matrixmetalloproteinases by mesenchymal stem/stromal cells

Gebraad, Arjen

2018-06

Gebraad , A , Kornilov , R , Kaur , S , Miettinen , S , Haimi , S , Peltoniemi , H , Mannerström , B & Seppänen-Kaijansinkko , R 2018 , ' Monocyte-derived extracellular vesicles stimulate cytokinesecretion and gene expression of matrixmetalloproteinases by mesenchymal stem/stromal cells ' , The FEBS Journal , vol. 285 , no. 12 , pp. 2337-2359 . https://doi.org/10.1111/febs.14485

http://hdl.handle.net/10138/303898
https://doi.org/10.1111/febs.14485

unspecified
publishedVersion

The FEBS Journal

FEBS PRESS science publishing by scientists

Monocyte-derived extracellular vesicles stimulate cytokine secretion and gene expression of matrix metalloproteinases by mesenchymal stem/stromal cells

Arjen Gebraad[1], Roman Kornilov[1], Sippy Kaur[1], Susanna Miettinen[2,3], Suvi Haimi[1], Hilkka Peltoniemi[4], Bettina Mannerström[1,†] and Riitta Seppänen-Kaijansinkko[1,†]

1 Department of Oral and Maxillofacial Diseases, Helsinki University Hospital, University of Helsinki, Finland
2 Adult Stem Cell Group, BioMediTech Institute, Faculty of Medicine and Life Sciences, University of Tampere, Finland
3 Science Center, Tampere University Hospital, Finland
4 Laser Tilkka Ltd, Helsinki, Finland

Keywords
cytokines; extracellular vesicles; mesenchymal stem/stromal cell; monocyte; osteoclast

Correspondence
A. Gebraad, Clinicum Department of Oral and Maxillofacial Diseases, Faculty of Medicine, University of Helsinki P.O. Box 41, Mannerheimintie 172, 00014 Finland
Tel: +358 504489496
E-mail: arjen.gebraad@helsinki.fi

[†]These authors contributed equally.

(Received 10 August 2017, revised 30 March 2018, accepted 20 April 2018)

doi:10.1111/febs.14485

Intercellular communication is essential in bone remodelling to ensure that new bone is formed with only temporary bone loss. Monocytes (MCs) and osteoclasts actively take part in controlling bone remodelling by providing signals that promote osteogenic differentiation of mesenchymal stem/stromal cells (MSCs). Extracellular vesicles (EVs) have attracted attention as regulators of bone remodelling. EVs facilitate intercellular communication by transferring a complex cargo of biologically active molecules to target cells. In the present study, we evaluated the potency of EVs from MCs and osteoclasts to induce a lineage-specific response in MSCs. We analysed gene expression and protein secretion by both adipose tissue-derived MSCs and bone marrow-derived MSCs after stimulation with EVs from lipopolysaccharide-activated primary human MCs and (mineral-resorbing) osteoclasts. Isolated EVs were enriched in exosomes (EVs of endosomal origin) and were free of cell debris. MC- and osteoclast-derived EVs were taken up by adipose tissue-derived MSCs. EVs from activated MCs promoted the secretion of cytokines by MSCs, which may represent an immunomodulatory mechanism. MC-derived EVs also upregulated the expression of genes encoding for matrix metalloproteinases. Therefore, we hypothesize that MCs facilitate tissue remodelling through EV-mediated signalling. We did not observe a significant effect of osteoclast-derived EVs on gene expression or protein secretion in MSCs. EV-mediated signalling might represent an additional mode of cell-cell signalling during the transition from injury and

Abbreviations
AT-MSC, adipose tissue-derived mesenchymal stem/stromal cell; BM-MSC, bone marrow-derived mesenchymal stem/stromal cell; CCL, chemokine [C–C motif] ligand; CXCL, chemokine [C–X–C motif] ligand; EV, extracellular vesicle; HA, hydroxyapatite; Hsp70, 70 kilodalton heat shock proteins; ICAM-1, intercellular adhesion molecule 1; LPS, lipopolysaccharide; MC-EV, extracellular vesicle from a lipopolysaccharide-activated monocyte; MC, monocyte; M-CSF, macrophage colony-stimulating factor; MM, maintenance medium; MSC, mesenchymal stem/stromal cell; OC HA-EV, extracellular vesicle from an osteoclast cultured on hydroxyapatite; OC TCPS-EV, extracellular vesicle from an osteoclast cultured on tissue culture polystyrene; OCDM, osteoclast differentiation medium; OC, osteoclast; ODM, osteogenic differentiation medium; PBMC, peripheral blood mononuclear cell; qPCR, quantitative PCR; RANKL, receptor activator of nuclear factor κ-B ligand; RANK, receptor activator of nuclear factor κ-B; SBF × 3, 3 × concentrated simulated body fluid; TCPS, tissue culture polystyrene; TRAcP, tartrate resistant acid phosphatase; TSG101, tumour susceptibility gene 101; UC LPS, ultracentrifugation precipitate from lipopolysaccharide-activation medium; UC OCDM, ultracentrifugation precipitate from lipopolysaccharide-supplemented osteoclast differentiation medium.

inflammation to bone regeneration and play an important role in the coupling between bone resorption and bone formation.

Database

Gene expression data are available in the GEO database under the accession number GSE102401.

Introduction

Cells release diverse types of membrane vesicles into the extracellular environment. These so-called extracellular vesicles (EVs) represent an important mode of intercellular communication by transferring a complex cargo of biologically active molecules to target cells [1,2]. Given the importance of cellular interactions in bone remodelling [3], EVs have attracted attention as regulators of this process [4]. EVs could find use in the treatment of bone diseases that are related to aberrant bone remodelling, such as rheumatoid arthritis, osteoarthritis and osteoporosis [5]. Moreover, EVs have potential in regenerative medicine as biomimetic tools to induce lineage-specific differentiation of stem cells [6,7]. The cell type from which the most potent regulatory EVs originate and the mechanism by which the EVs mediate bone remodelling remain to be investigated [5,8].

The immune system strongly influences tissue repair and regeneration, and active control of the immune system is an attractive therapeutic approach to induce tissue regeneration [9], including bone regeneration [10]. The mononuclear phagocytic system is part of the immune system and consists of hematopoietic cells derived from progenitor cells in the bone marrow (BM) [11]. Monocytes (MCs) and osteoclasts (OCs) are mononuclear phagocytic cell types that share precursors. Both MCs [12,13] and OCs [14–16] actively take part in controlling bone remodelling by providing signals that promote osteogenic differentiation of mesenchymal stem/stromal cells (MSCs).

In the context of tissue healing, there are few studies looking into the potential of EVs from mononuclear phagocytes. Nevertheless, EVs from these cells most likely have a role in the crosstalk between immunity and tissue healing [17] and may contribute to maintaining bone homeostasis [4]. In the present study, we evaluated the potency of EVs from primary human MCs and OCs to induce a lineage-specific response in MSCs. We analysed gene expression and protein secretion by both adipose tissue-derived MSCs (AT-MSCs) and BM-derived MSCs (BM-MSCs) after stimulation with EVs from activated primary human MCs and OCs. The study sheds light on the mechanism by which EVs mediate bone remodelling and their potential as therapeutic tools to enhance the regeneration of bone tissue.

Results

Culture of lipopolysaccharide-activated monocytes and formation of osteoclasts on tissue culture plastic and hydroxyapatite coatings

Monocyte and OC cultures were monitored using a phase-contrast microscope (Fig. 1). Lipopolysaccharide (LPS)-activated MCs were visible as small adherent cells. The conditioned medium from these cells was collected at 3 days (Fig. 1A,B) and 5 days (Fig. 1C) of culture. Part of the LPS-activated MCs was positive for OC-marker tartrate resistant acid phosphatase (TRAcP; Fig. 1B).

One of the aims of this study was to investigate the effect of OC-EVs on the differentiation of MSCs. Therefore, peripheral blood MCs were differentiated towards OCs using macrophage colony-stimulating factor (M-CSF) and receptor activator of nuclear factor κ-B ligand (RANKL). MCs eventually fused and formed OCs in presence of M-CSF and RANKL (Fig. 1D,E). Nonactive OCs were generated on tissue culture plastic (tissue culture polystyrene, TCPS). Henriksen *et al*. [16] showed that pro-osteogenic signalling of OCs is partially dependent on mineral dissolution. To investigate if the potential EV-signalling from OCs to MSCs is dependent on mineral dissolution, cells were also cultured on a hydroxyapatite (HA) substrate (Fig. 1H–K). HA coatings have been previously used to model mineral dissolution by OCs [18,19]. The formation of mature OCs was confirmed by the positive staining for TRAcP (Fig. 1F). Mature OCs on HA were dissolving the substrate (Fig. 1K,J).

Characterization of EVs from LPS-activated monocytes and osteoclasts

Extracellular vesicles were obtained using an isolation kit or by ultracentrifugation (UC) of the MC- and OC-conditioned medium. The obtained particles were

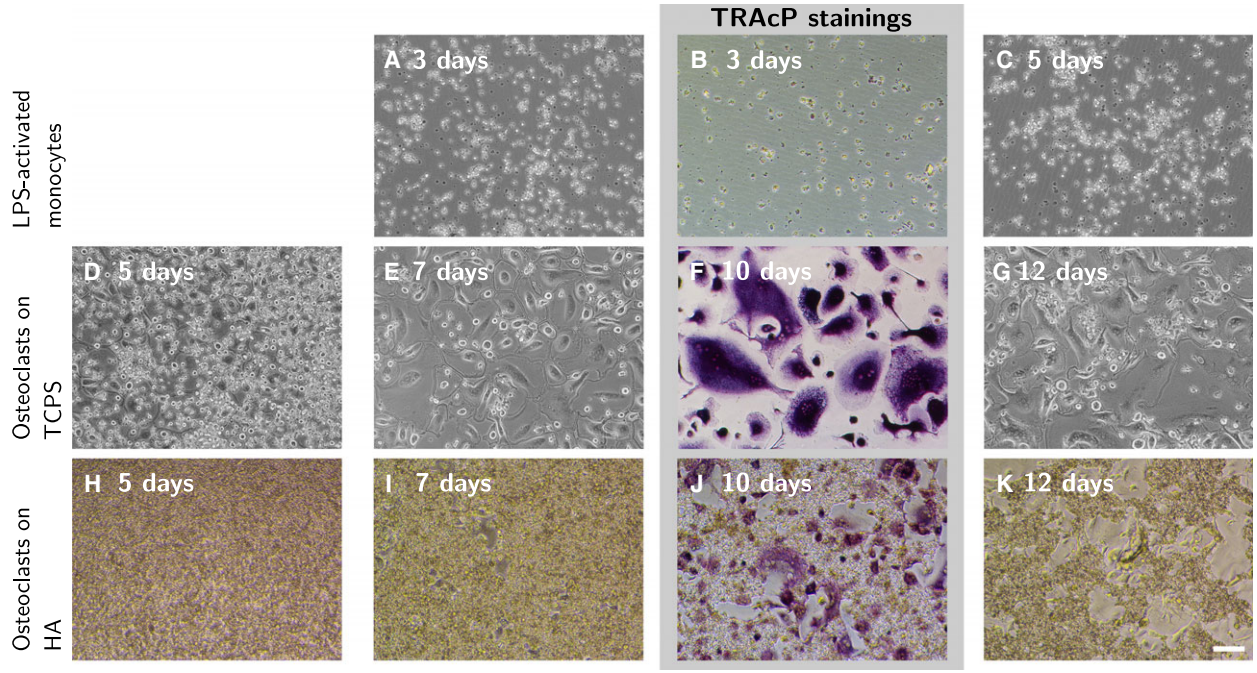

Fig. 1. Phase-contrast microscopy (A,C–E,G–I,K) and stainings for osteoclast-marker TRAcP (B,F,J) of LPS-activated MCs (A–C), osteoclasts on TCPS (D–G) and osteoclasts on HA coatings (H–K). MC-conditioned medium was collected at 3 days (A,B) and 5 days (C) of culture. Incomplete osteoclast formation (D) and intact HA coating (H) was observed at 5 days of osteoclast differentiation. Medium was changed to medium depleted of EVs when osteoclasts had formed (E,I). Osteoclast-conditioned medium was collected 3 days (F,J) and 5 days (G,K) after changing to EV-depleted medium. Scale bar: 100 μm.

characterized for size, morphology and the presence or absence of membrane proteins. Transmission electron microscopy revealed the isolation of vesicles with an intact lipid bilayer (Fig. 2A–F).

Nanoparticle tracking analysis showed that the large majority (> 80%) of the particles isolated in this study was between 50 and 200 nm in diameter (Fig. 3). The number of particles between 50 and 400 nm in diameter were considered EVs for the functional assays in this study. Isolation using the kit resulted in a higher number of EVs than isolation by UC (Table 1), especially from OCs cultured on TCPS. The number of EVs recovered from MC-conditioned medium by UC did not reach beyond the background levels of unconditioned LPS-supplemented medium. UC yielded bigger EVs, especially for MCs.

Western blotting revealed the presence of EV-associated proteins CD90 (Thy-1), tumour susceptibility gene 101 (TSG101) and 70 kilodalton heat shock proteins (Hsp70; Fig. 4). TSG101 and Hsp70 were also detected from MC lysate. CD63 (lysosomal-associated membrane protein 3), a marker for EVs of endosomal origin was only barely detectable extracellular vesicles from lipopolysaccharide-activated MCs (MC-EVs). CD63 was on the other hand highly enriched in EVs from OCs cultured on both TCPS (OC TCPS-EVs) and HA coatings (OC HA-EVs). MC and macrophage marker CD14 was present in all EV types, just like RANKL receptor RANK. The CD14 and RANK signals were minute in MC lysate. Calnexin, a protein of the endoplasmic reticulum, was only present in MC lysate.

Uptake of EVs by adipose tissue-derived-mesenchymal stem/stromal cells

To show that the MC-EVs and OC-EVs could interact with MSCs, we studied the uptake of the EVs by AT-MSCs (Fig. 5). EVs were labelled with lipophilic dye DiD before adding them to AT-MSC cultures. After 3 days of culture, labelled EVs from all three cell sources were visible inside the AT-MSCs (Fig. 5B–D). To exclude that DiD micelles or other background staining would be mistaken for EVs, EV-free PBS was stained with DiD and processed the same way. No background staining was visible under the confocal microscope when the cells had been incubated with the control (Fig. 5A).

The interaction between AT-MSCs and MC-EVs and OC-EVs was confirmed by flow cytometry analysis (Fig. 5E–G). EV-positive AT-MSC fractions could be

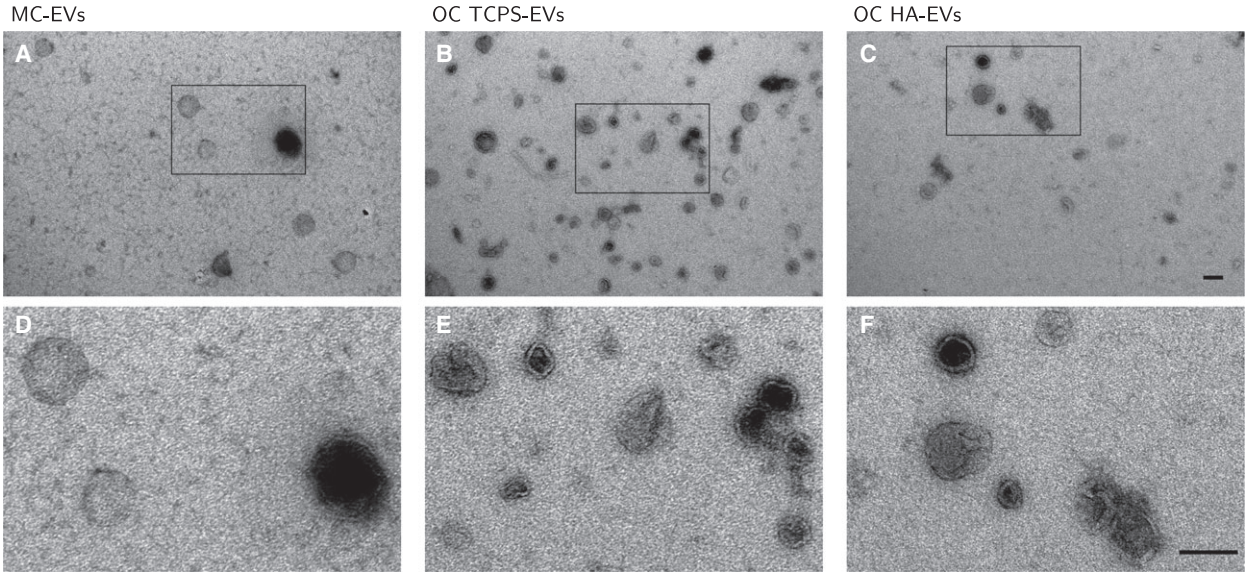

Fig. 2. Transmission electron microscopy images of MC-EVs (A,D), OC TCPS-EVs (B,E) and OC HA-EVs (C,F). Close-ups (D,E,F) of the regions marked in A, B and C, respectively. Scale bars: 100 nm.

Table 1. EV yield and median particle size based on nanoparticle tracking analysis.

EV source	Median size (Q1–Q3)	Yield·mL^{-1} of conditioned medium
LPS-activated MCs		
Donor 1	107 nm (86–158)	1.43×10^{9}
Donor 2	91 nm (77–124)	1.68×10^{9}
Donor 3	133 nm (107–198)	3.56×10^{8}
Donor 4	147 nm (112–193)	3.17×10^{8}
Osteoclasts on TCPS		
Donor 1	114 nm (92–149)	1.17×10^{10}
Donor 2	126 nm (98–163)	1.96×10^{10}
Donor 3	134 nm (112–165)	7.42×10^{8}
Donor 4	131 nm (108–163)	5.40×10^{8}
Osteoclasts on HA		
Donor 1	126 nm (96–155)	2.35×10^{9}
Donor 2	121 nm (93–157)	6.03×10^{9}
Donor 3	120 nm (97–155)	1.24×10^{8}
Donor 4	135 nm (112–170)	7.87×10^{8}

detected, defined as the fraction of the cells with a fluoresence higher than greater than that of 95% of AT-MSCs incubated with the DiD-labelled control.

Microarray analysis of gene expression by AT-MSCs cultured in the presence of monocyte- and osteoclast-derived EVs

The effect of the MC-EVs and OC-EVs on gene expression patterns in AT-MSCs was analysed using microarrays. AT-MSCs were exposed to equal numbers of MC-EVs or OC-EVs for a period of 18 days. The EVs had been isolated from the conditioned media using the isolation kit. AT-MSCs cultured in EV-depleted maintenance medium (MM) was the reference condition. Because gene expression patterns related to osteoblast differentiation and bone remodelling were of interest in this study, we also included AT-MSCs cultured in established osteogenic culture conditions (osteogenic differentiation medium, ODM).

A total of 3187 genes were found to be differentially expressed between the culture conditions (false discovery rate < 0.05; Figs 6 and 7). We performed direct quantification of nine selected gene transcripts by quantitative PCR (qPCR) to validate the microarray findings (Fig. 8). The qPCR analysis was performed separately for each of the six donor replicates. In every case, a strong correspondence between the microarray and qPCR data was observed.

Figure 6 shows a heatmap of the genes that were differentially expressed between the culture conditions. Gene expression patterns of samples cultured in ODM were most distinct from those in other conditions. However, ODM did not result in a gene expression pattern typical of (differentiating) osteoblasts. Osteogenic marker genes like *RUNX2* or *ALPL* stayed at similar or even slightly lower levels, although not significant. Expression of *BMP2*, which plays an important role in bone development, was even substantially downregulated in ODM. When the microarray results were validated by qPCR, *BMP2*

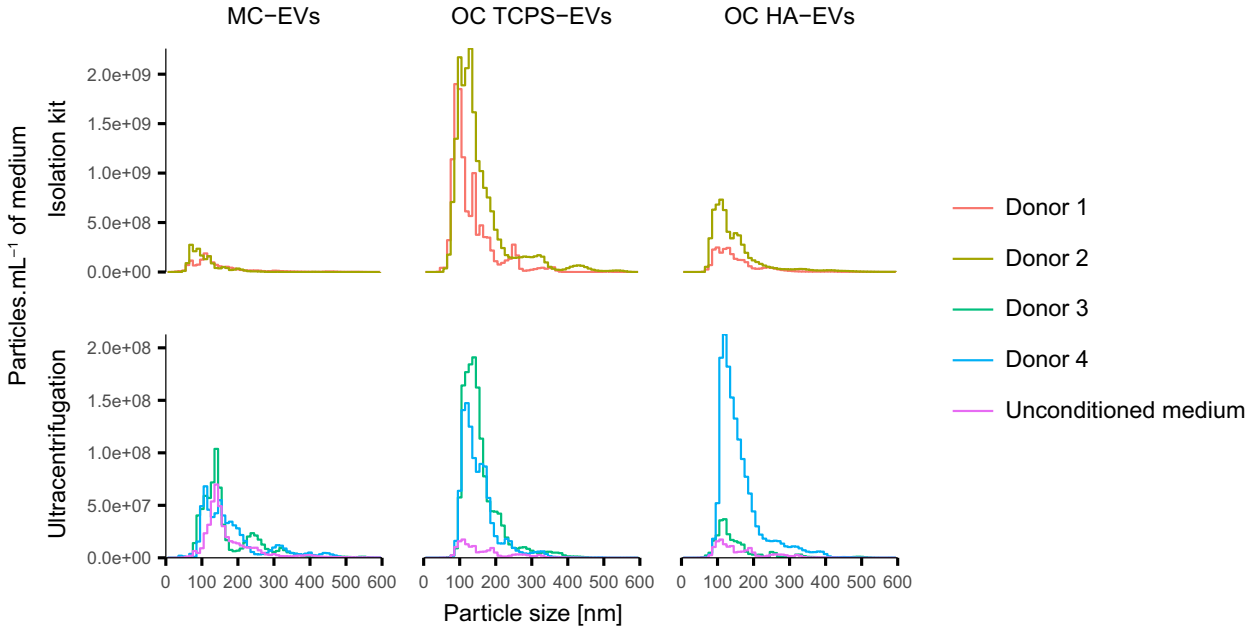

Fig. 3. Distribution of particles in MC-EVs, OC TCPS-EVs and OC HA-EVs according to nanoparticle tracking analysis. Particles were isolated using the EV isolation kit for blood donors 1 and 2 and by UC for blood donors 3 and 4. UC precipitate from LPS-activation medium and LPS-supplemented OCDM that had not been in touch with cells (unconditioned medium) were included as negative controls for MC-EVs and OC-EVs, respectively. Particle concentration in each bin (10 nm in size) is expressed as the number of particles·mL^{-1} of (un)conditioned medium from which the particles originate.

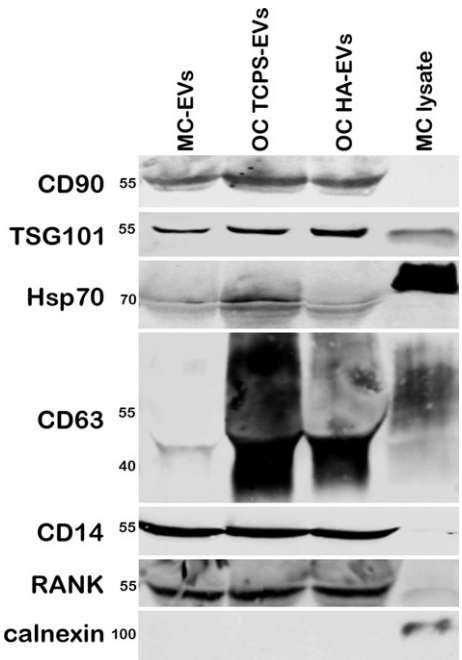

Fig. 4. Western blots for EV-associated proteins CD90, TSG101, CD63 and Hsp70, MC and macrophage marker CD14, RANKL receptor RANK and endoplasmic reticulum protein calnexin in EVs and MC lysate.

expression levels were significantly lower in ODM compared to MM (Fig. 8).

The gene expression patterns of cells from donor pool was similar when these cells had been exposed to OC TCPS-EVs, OC HA-EVs or when cultured in MM without EVs (Fig. 6). The gene expression patterns were more similar between these conditions than with other donor pools in the same culture condition. This reflects the similarity between these conditions and the limited effect of OC-EVs on gene expression patterns in AT-MSCs. Exposure to either OC TCPS-EVs or OC HA-EVs, did not lead to significant regulation of genes relative to EV-depleted MM (Fig. 7).

Stimulation with MC-EVs on the other hand resulted in 176 upregulated genes and 251 downregulated genes compared to EV-depleted MM (Fig. 7). Samples exposed to MC-EVs show great similarity among the different donor pools (Fig. 6). Genes that were differentially expressed in the presence of MC-EVs showed great overlap with genes differentially expressed in established osteogenic induction conditions. Of the 427 genes that were significantly regulated by MC-EVs, 211 were also differentially expressed in ODM. The direction of regulation, however, did not necessarily match. Of the 176 genes upregulated by MC-EVs, only 10 were also

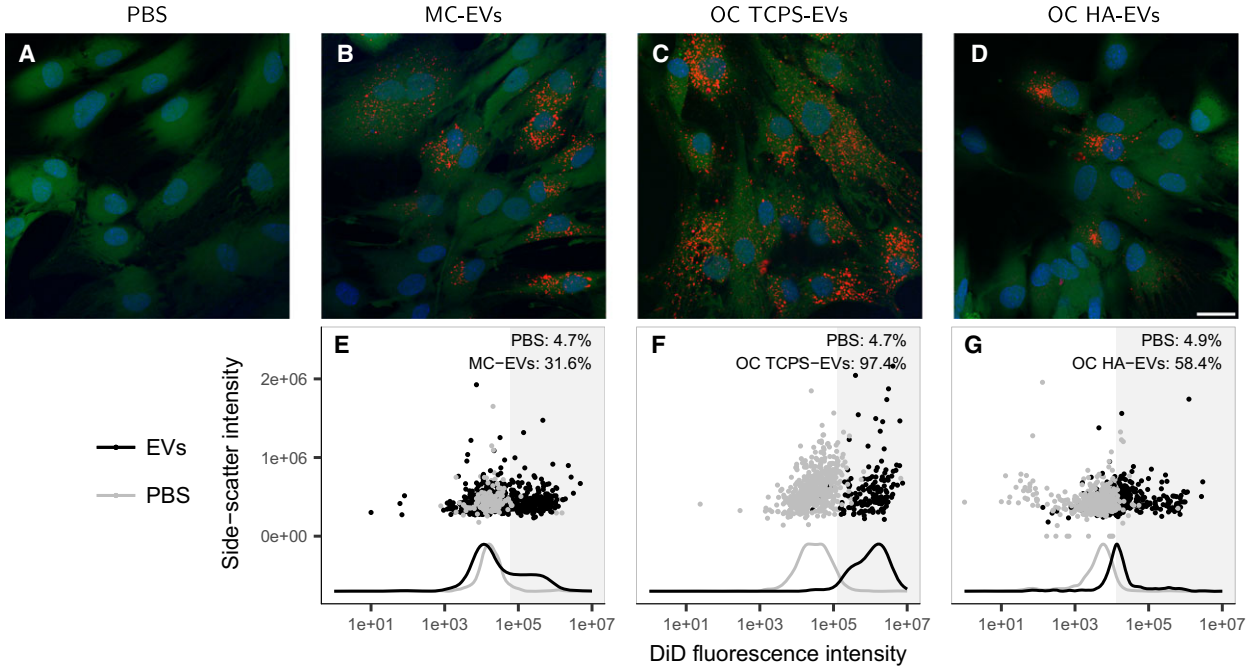

Fig. 5. EVs were added to cultures of AT-MSCs and uptake was examined after 72 h using confocal microscopy (A–D) and flow cytometry (E–G). AT-MSCs were cultured with EV-free PBS control (A), with MC-EVs (B,E), OC TCPS-EVs (C,F) and OC HA-EVs (D,G), all stained with lipophilic dye DiD. Blue: Hoechst 33342-stained nuclei, green: CellTrace™ CFSE-stained cell membrane, red: DiD-labelled EVs. Scale bar: 25 μm. Percentages denote DiD-positive fraction (grey area) in flow cytometry analysis with 5% overlap with cells cultured in PBS control.

upregulated in ODM and 53 genes were downregulated in ODM. Of the 251 genes downregulated by MC-EVs, 107 were also downregulated in ODM and 41 were upregulated.

Genes that were significantly upregulated by MC-EVs include many genes encoding for cytokines (Fig. 9). More specifically, CXC chemokines, such as *CXCL5* and *CXCL3*, and interleukin 1 (IL-1) cytokines, such as *IL1RN* and *IL1B* were expressed at higher levels. In addition, exposure to MC-EVs led to expression levels of matrix metalloproteinases, such as *MMP3* and *MMP1*.

To characterize the function of the genes upregulated by MC-EVs, an enrichment analysis of the genes was performed by their functional annotation with gene ontology (Fig. 10). Gene ontology terms for biological processes reflecting the function of cytokines, such as regulation of cell motility, positive regulation of cell migration and positive regulation of immune system processes were enriched for genes upregulated by MC-EVs. Gene ontology terms for molecular functions exerted by cytokines and chemokines in particular were enriched, as well as the binding of receptors for CXCR chemokines and IL–1 molecules. Enrichment of the gene ontology term for metalloendopeptidase activity reflects the increased expression levels of matrix metalloproteinases.

Biochemical analysis of AT-MSCs cultured in the presence of monocyte- and osteoclast-derived EVs

Quantification of alkaline phosphatase activity was employed to evaluate the effect of MC-EVs or OC-EVs on the early osteogenic differentiation of AT-MSCs (Fig. 11). The observed effect of established osteogenic conditions was only small. Exposure to MC-EVs led to a slightly bigger increase in alkaline phosphatase activity. We did not observe an effect of OC TCPS-EVs or OC HA-EVs on alkaline phosphatase activity.

Total collagen production was evaluated by quantification of hydroxyproline content in the cell lysate. ODM induced a small median increase in collagen production compared to EV-depleted MM. Collagen content had increased substantially under OC HA-EVs stimulation for some samples. The effect from MC-EVs was more consistent among the different donor replicates causing a median 2-fold increase in collagen content. We observed a slight decrease in collagen content when OC TCPS-EVs were used to stimulate AT-MSCs.

According to Kruskal–Wallis one-way analysis of variance by ranks, alkaline phosphatase activity and collagen content were not equal in all conditions ($P = 0.021$ and $P = 0.0098$, respectively).

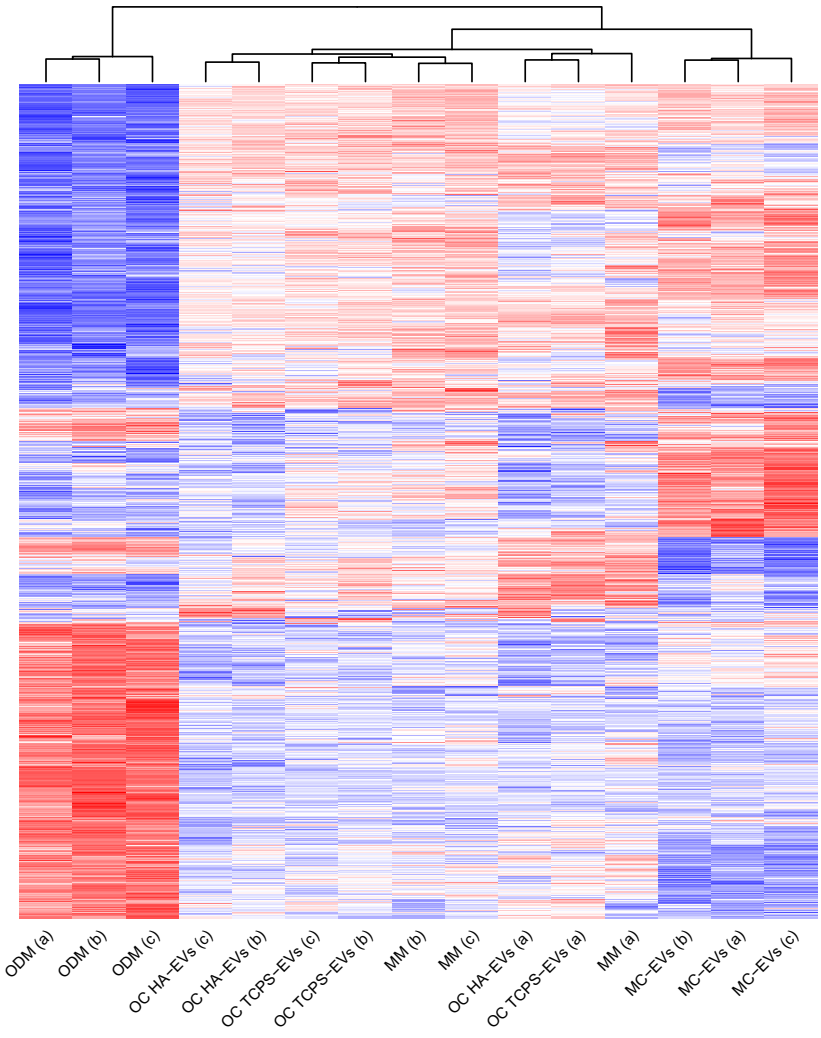

Fig. 6. Heat map generated from microarray data reflecting the *Z*-score of gene expression values of AT-MSCs cultured in EV-depleted MM, ODM or MM supplemented MC-EVs, OC TCPS-EVs or OC HA-EVs. Red denotes high gene expression and blue denotes low gene expression. The microarray was performed using three distinct pools per condition (a,b and C), assembled from five donor cell replicates. The dendogram illustrates the arrangement of clusters produced by hierarchical clustering.

Gene expression and protein secretion by AT-MSCs and BM-MSCs cultured in the presence of monocyte- and osteoclast-derived EVs

Next, we assessed the difference between MSCs isolated from adipose tissues and BM with respect to their response to MC- and OC-EVs. LPS was added to both MCs and OCs before the conditioned medium was collected. EVs were isolated by UC. To control for the effect of particles coprecipitated with the EVs, we supplemented the MSC culture medium with UC precipitate from LPS-activation medium (UC LPS) and LPS-supplemented osteoclast differentiation medium (UC OCDM) that had not been in touch with cells. After culturing the AT-MSCs and BM-MSCs in the presence of the EVs and controls without EVs, we analysed gene expression using qPCR (Fig. 12). Genes were chosen because of their relevance in osteoblast differentiation or because they had been found differentially expressed in MC-EV-stimulated AT-MSCs in our microarrays. In addition, we assessed the secretion of cytokines and soluble intercellular adhesion molecule 1 (ICAM-1) at protein level (Fig. 13).

These experiments confirmed in large the results obtained from the microarrays. Expression of *CXCL5* was increased in the presence of MC-EVs for both AT-MSCs and BM-MSCs (Fig. 12A). The difference with UC LPS was statistically significant for BM-MSCs. *MMP1* expression levels were also slightly increased in AT-MSCs in response to MC-EVs (Fig. 12B). We did not detect differences in *MMP1* expression levels in BM-MSCs in response to EVs. *MMP1* expression by BM-MSCs was substantially decreased when BM-MSCs were cultured in ODM. Culture in ODM slightly decreased expression levels of *ICAM1* in AT-MSCs (Fig. 12C), confirming our previous observation (Fig. 8F). In BM-MSCs on the other hand, *ICAM1* was expressed at significantly higher

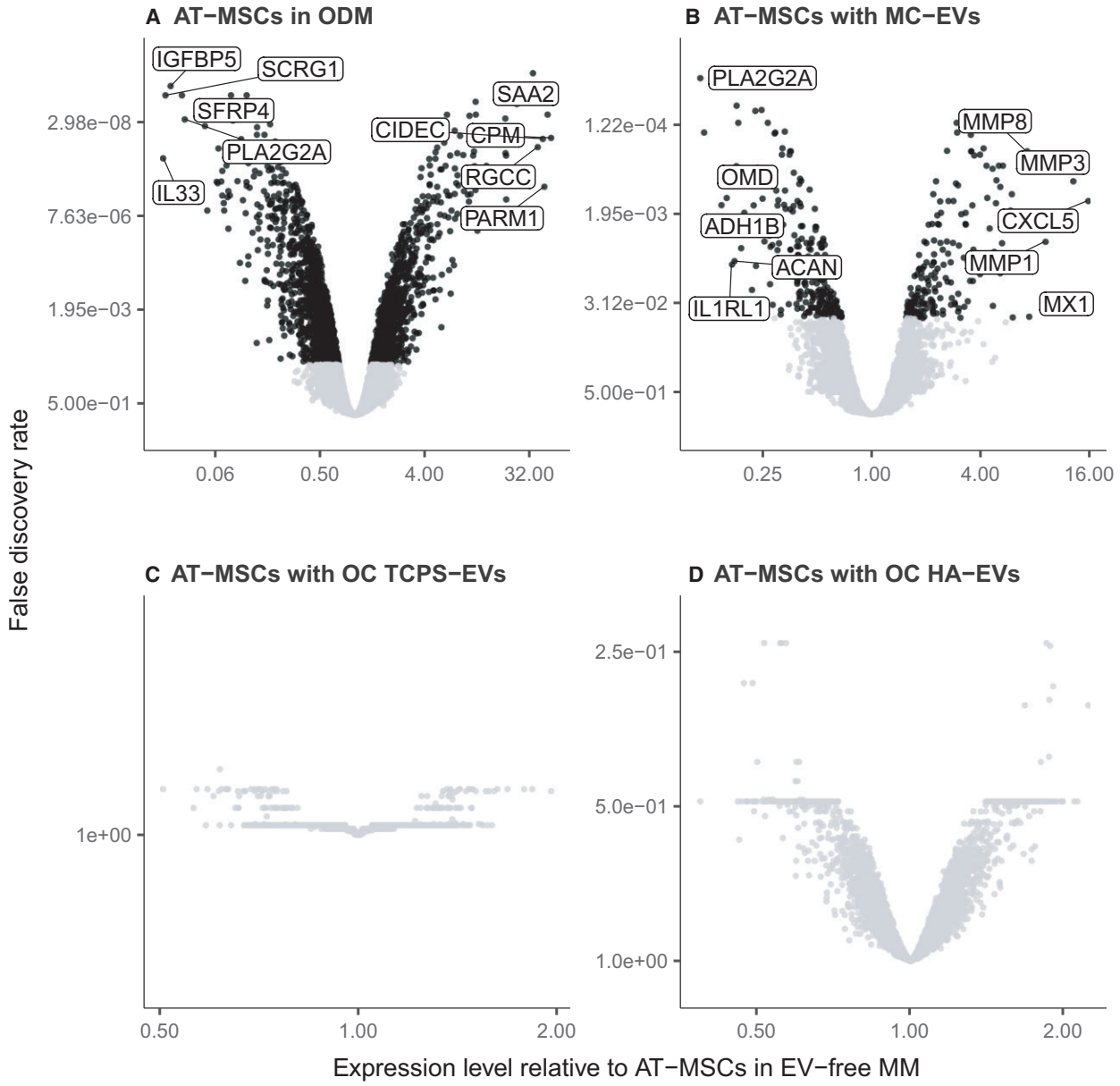

Fig. 7. Vulcano plots of gene expression by AT-MSCs cultured in ODM (A) or exposed to MC-EVs (B), OC TCPS-EVs (C) or OC HA-EVs (D), according to microarray analysis. Statistical significance (as false discovery rate in reversed log2 scale) is plotted against the fold change (log2 scale) with AT-MSCs cultured in EV-free MM. Genes indicated as black dots are significantly differentially expressed based on moderated paired *t*-tests and by controlling the false discovery rate (< 0.05). Five most up- and -downregulated genes are indicated.

levels in ODM than in MM. *ICAM1* expression was higher in the presence of EVs than in MM for both MSC types, but a similar effect was seen in AT-MSCs when cultured with UC precipitate without EVs. Stimulation of BM-MSCs with MC-EVs and OC TCPS-EVs caused a substantial increase in expression of *ICAM1* compared to the controls without EVs. Expression of osteogenic marker genes *ALPL* and *RUNX2* were not affected by our experimental conditions (Fig. 12D,E). BM-MSCs expressed *RUNX2* at higher levels than AT-MSCs.

Monocyte-EVs stimulated the secretion of cytokines by AT-MSCs, confirming our microarray results (Fig. 13A–C). MC-EVs also increased cytokine secretion by BM-MSCs, although the effect was less apparent than for AT-MSCs. Due to the high variability between the three donor repeats, no statistically significant differences were found between the protein

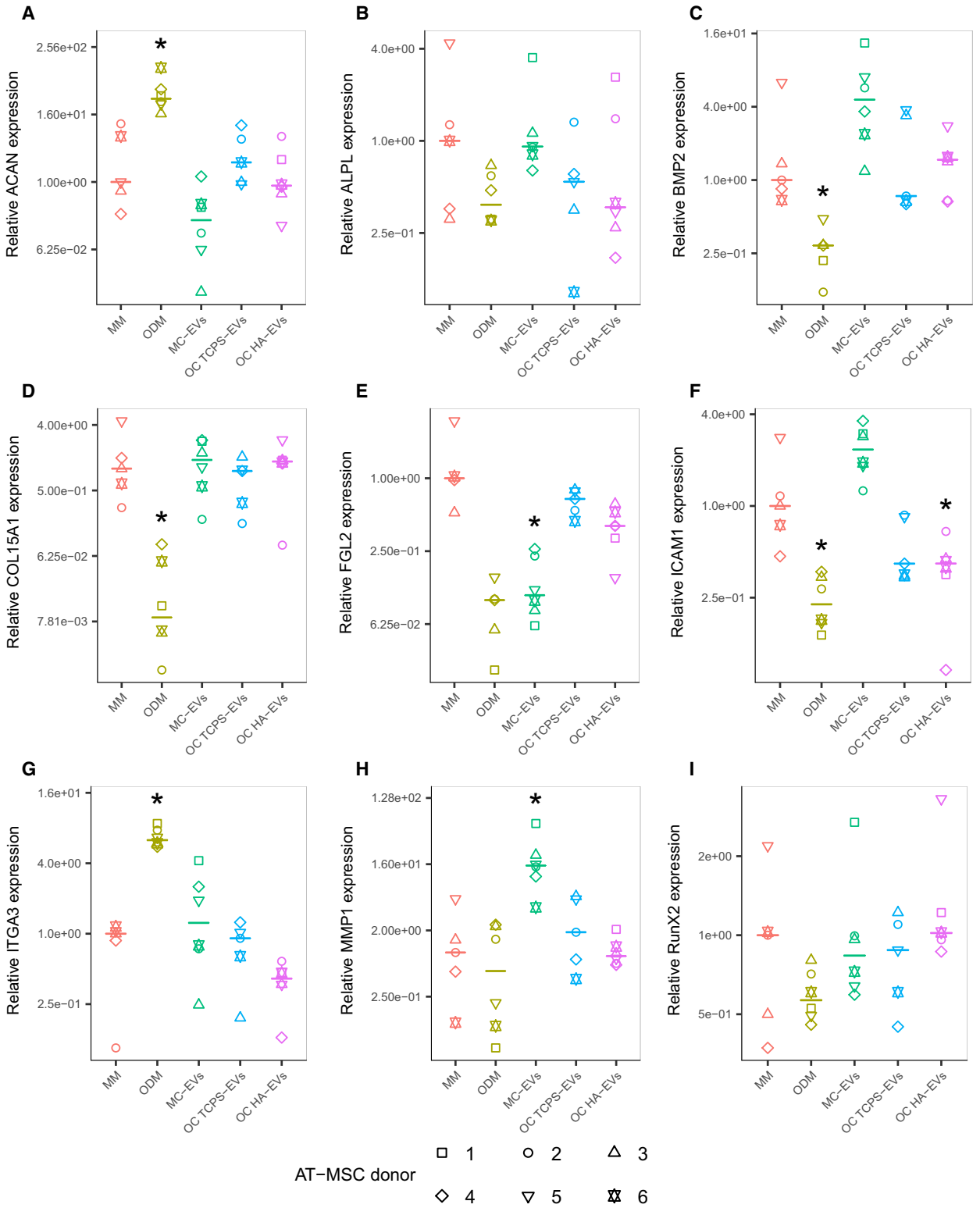

Fig. 8. Quantitative PCR analysis of gene expression of *ACAN* (A), *ALPL* (B), *BMP2* (C), *COL15A1* (D), *FGL2* (E), *ICAM1* (F), *ITGA3* (G), *MMP1* (H) and *RUNX2* (I) in AT-MSCs cultured in EV-free MM, EV-free ODM or AT-MSCs exposed MC-EVs, OC TCPS-EVs or OC HA-EVs. Gene expression levels (log2 scale) are shown relative to the median gene expression in MM. *False discovery rate-controlled *P*-value < 0.05, based on Mann–Whitey *U*-tests with MM. [Colour figure can be viewed at wileyonlinelibrary.com]

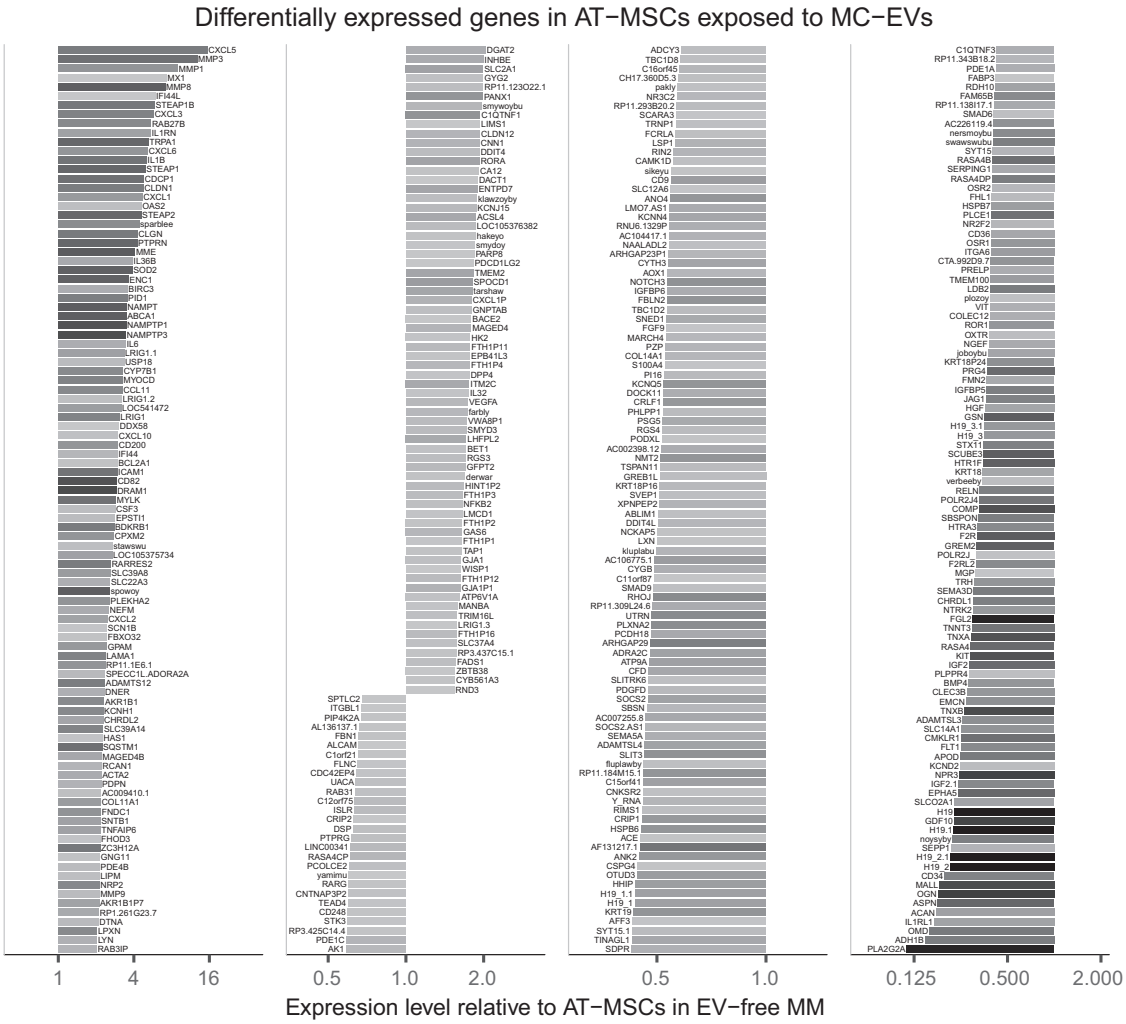

Fig. 9. Differentially expressed genes in AT-MSCs exposed to MC-EVs according to microarray analysis. Bars indicate gene expression levels (log2 scale) relative to AT-MSCs in EV-free MM. Darker shade of the bar denotes higher statistical significance of the difference with MM based on a moderated paired *t*-test and false discovery rate controlling procedures.

secretion by MSC-EV-stimulated AT-MSCs and the control (UC LPS). The conditioned medium from MSCs cultured with OC TCPS-EVs also contained slightly elevated levels of cytokines. The chemokines CCL2 (chemokine [C–C motif] ligand 2) and IL8 were already present in the OC TCPS-EV-supplemented medium. Chemokines CCL5, chemokine [C–X–C motif] ligand 9 (CXCL9) and CXCL10 were not detected by the human chemokine kit.

Mesenchymal stem/stromal cells secreted soluble ICAM-1 in response to MC-EVs and OC-EVs (Fig. 13D). ICAM-1 secretion in response to the EVs showed similarities with cytokine secretion. AT-MSCs secreted the most ICAM-1 in response to MC-EVs, just like we observed for cytokines. Highest ICAM-1 concentrations in BM-MSC-conditioned medium were measured from cultures with OC-TCPS-EVs, but like cytokines, soluble ICAM-1 was already present in the OC TCPS-EV-supplemented medium before MSCs were cultured.

Discussion

Tight control of bone remodelling through cellular interactions is essential to ensure that new bone is formed with only temporary bone loss. Many cell types and molecular mechanisms contribute to coupling between bone resorption and bone formation [3]. EVs from mononuclear phagocytes most likely have a role in maintaining bone homeostasis [17]. EVs from LPS-activated MCs for instance, were found to increase expression levels of osteogenic marker genes *RUNX2*,

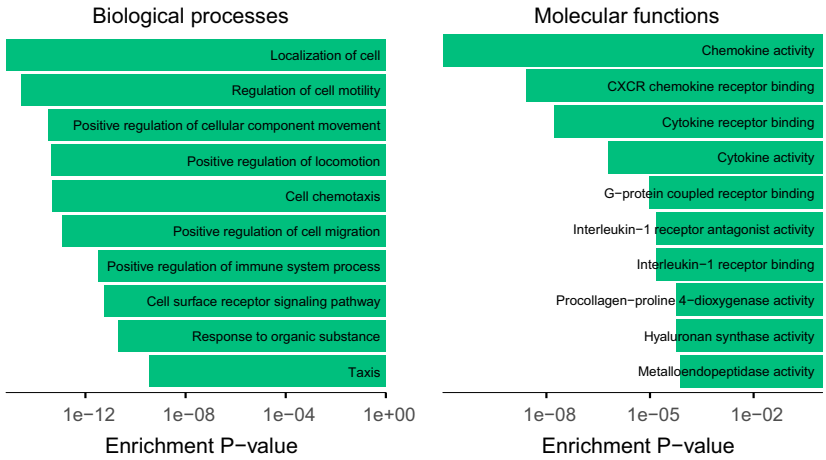

Fig. 10. Gene ontology terms for biological processes and molecular functions that are most enriched for genes significantly upregulated by MC-EVs. Enrichment *P*-values in log2 scale.

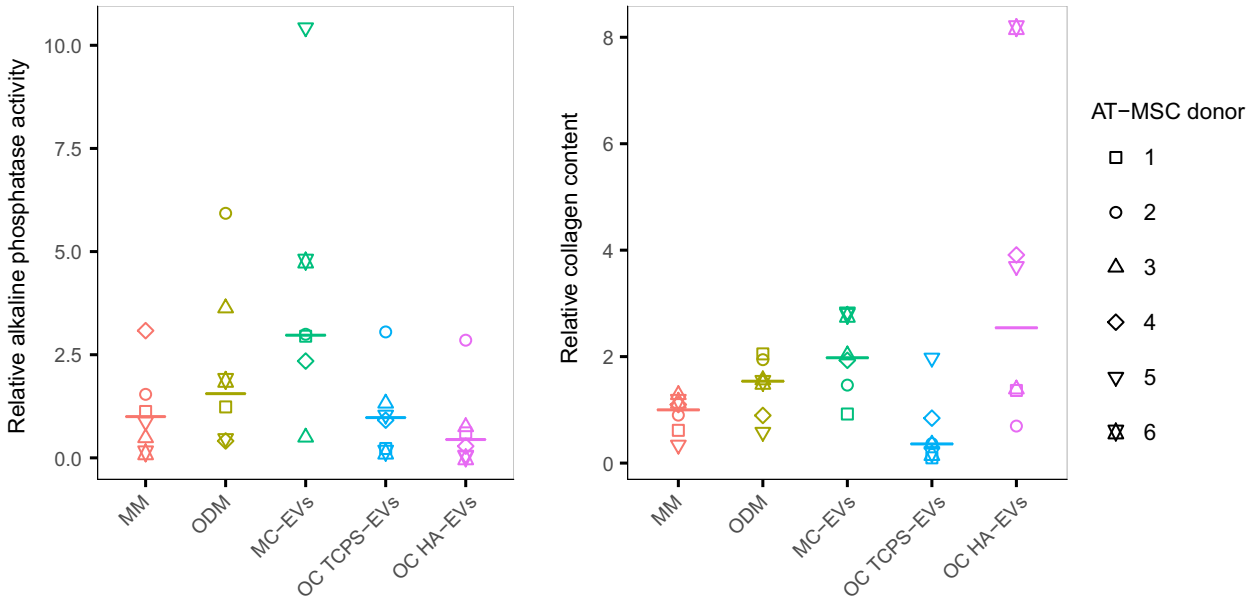

Fig. 11. Relative alkaline phosphatase activity and total collagen content in AT-MSCs cultured in EV-depleted MM, EV-depleted ODM or MM supplemented with MC-EVs, OC TCPS-EVs or OC HA-EVs. Results are normalized for cell number and expressed relative to the median in MM.

BMP2 and *BGLAP* and were suggested to constitute an additional mode of cell-cell signalling during the transition from injury and inflammation to bone regeneration [20]. OCs couple their bone-resorbing activity to the activity of osteoblasts by providing signals that promote osteogenic differentiation of MSCs and coordinate osteoblastic bone formation [14–16]. We wanted to find out if the osteoinductive signals from OCs to MSCs are partially carried by EVs.

We compared the effects of EVs from LPS-activated MCs and OCs at a genome-wide scale. Unlabelled MCs were obtained by depletion of non-MCs using a cocktail of antibody-conjugated microbeads. Positive selection of CD14+ MCs using anti-CD14 microbeads would block CD14, which functions as a receptor for LPS [21]. This would lead to an inability of the MCs to be activated by LPS stimulation, which is thought to lead to more profound and prolonged osteoinductive signalling to MSCs [22]. When experiments were repeated, we also added LPS to the OC cultures to make comparison between the effects of MC-EVs and OC-EVs more straightforward. We hypothesized that EVs represent a part of the osteoinductive signals from OCs to MSCs that depends on the resorption activity

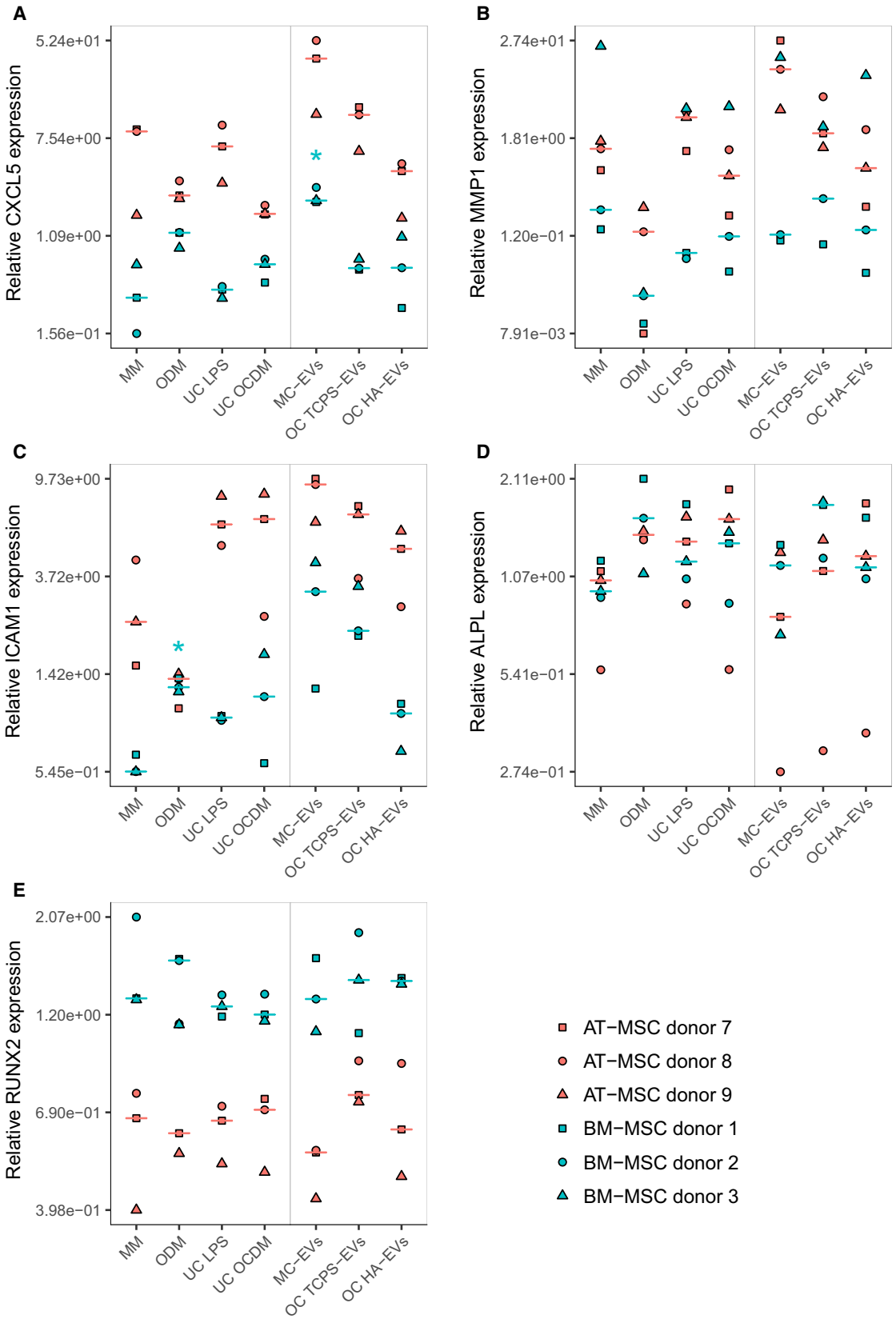
A
Relative CXCL5 expression
5.24e+01
7.54e+00
1.09e+00
1.56e−01
B
Relative MMP1 expression
2.74e+01
1.81e+00
1.20e−01
7.91e−03
C
Relative ICAM1 expression
9.73e+00
3.72e+00
1.42e+00
5.45e−01
D
Relative ALPL expression
2.11e+00
1.07e+00
5.41e−01
2.74e−01
E
Relative RUNX2 expression
2.07e+00
1.20e+00
6.90e−01
3.98e−01
MM
ODM
UC LPS
UC OCDM
MC−EVs
OC TCPS−EVs
OC HA−EVs
AT−MSC donor 7
AT−MSC donor 8
AT−MSC donor 9
BM−MSC donor 1
BM−MSC donor 2
BM−MSC donor 3

Fig. 12. Quantitative PCR analysis of gene expression of *CXCL5* (A), *MMP1* (B), *ICAM1* (C), *ALPL* (D) and *RUNX2* (E) in AT-MSCs (pink fill) and BM-MSCs (blue fill). MSCs were cultured in EV-free MM, ODM or exposed to MC-EVs, OC TCPS-EVs or OC HA-EVs. In addition, MSCs were cultured in MM supplemented with UC LPS or UC OCDM. Gene expression levels (log2 scale) are shown relative to the median gene expression in MM. Pink and blue bars indicate median expression for AT-MSCs and BM-MSCs, respectively. *False discovery rate-controlled *P*-value < 0.05, based on paired *t*-tests for *CXCL5* expression in BM-MSCs between MC-EVs and UC LPS (A) and for *ICAM1* expression in BM-MSCs between ODM and MM (C).

by OCs [16]. Mineral resorbing OCs were therefore included as an EV source. OCs were activated for mineral resorption by culturing them on coatings of HA.

EV isolation method affected EV yield, but did not change the response in MSCs

We used a kit to isolate the EVs from the cell-conditioned medium for the microarray experiments. The isolation kit works by lowering the hydration of the EVs, thereby reducing their solubility and allowing precipitation of the EVs at lower centrifugal forces. The main advantage of this type of kits is the ability to isolate EVs from a large volume of conditioned medium in a relatively short period of time. However, these kits usually give lower purity than e.g. UC, as the solubility of almost all particles decreases equally [23]. When we repeated the experiments and included BM-MSCs exposed to the EVs, we had isolated the EVs by UC. The particle yield in the UC precipitate was much lower than in the kit's isolate (Fig. 3 and Table 1). It is possible that most particles isolated using the kit were not EVs. Nevertheless, experiments using kit isolates and using EVs obtained by UC lead to similar results. We included EV-free controls for UC and obtained relatively high background levels. The effects of coprecipitated particles on gene expression and cytokine secretion by MSCs, though, were still minor compared to the effects of the EVs, especially MC-EVs.

More EVs were obtained from OCs on TCPS, with the exception of blood donor 4. The higher yield from OCs on TCPS than on the HA coatings could be explained by better attachment of the cells on TCPS, resulting in higher cell proliferation than on HA. Consequently, more cells were available to produce EVs.

EV isolates were enriched in exosomes and were free of cell debris

Detection and characterization of EVs in a standardized manner have proven difficult [24]. EV are therefore often characterized using a combination of methods. We identified EVs based on their size, presence of proteins and their biological activity according to the minimal criteria parameters recommended by the International Society of EVs [25]. Overall, morphology and size distribution of the particles indicated an enrichment in exosomes, EVs of endosomal origin between 40 and 100 nm in diameter [26].

The presence of CD90 argues for the presence of membrane in the isolate and is a general EV marker [25] (Fig. 4). EVs can bear Hsp70 when they are exposed to stress conditions [27], and could be upregulated upon LPS stimulation [28]. The presence of TSG101 is more specific for exosomes: TSG101 is required for the sorting of cargo into exosomes [29]. Interestingly, there was a strong signal from tetraspanin CD63 in OC-EVs, while it was almost absent in MC-EVs. Tetraspanins are widely used as exosome markers, because of their role in biogenesis, assembly, and sorting of protein and genetic material into exosomes [27]. Our other results do, however, not suggest a shift in EV population from microvesicles to exosomes when MCs differentiate towards OCs. This shows the difficulty in finding common EV/exosome marker proteins for EVs derived from different cell types, even if those cells stem from the same population.

Monocyte-EVs and OC-EVs were both positive for CD14, reflecting the cell membrane of the MC and shows that CD14 is still expressed on the EV surface once MCs have differentiated into OCs. In accordance with Huynh *et al.* [30], we detected RANK in the EVs from mature OCs. The RANK-rich EVs may function by competing with RANK+ OC precursors for RANKL, thereby inhibiting their own formation [30]. The MC-EVs also expressed RANK, contrary with the previously reported RANK-negative EVs from primary mouse marrow-derived OC precursors [30]. This shows that precursor cells derived from different tissues and animals might differ in the EVs they produce and the way these EVs function in regulating differentiation.

As mentioned above, impurities in the samples might affect the results. We can rule out major contaminations consisting of cell debris, because endoplasmic reticulum protein calnexin was absent.

Isolated monocyte- and osteoclast-derived EVs were functional and adipose tissue-derived MSCs are one of their targets

Apart from sample purity, it is important that the isolated EVs are functional. Our results show that the

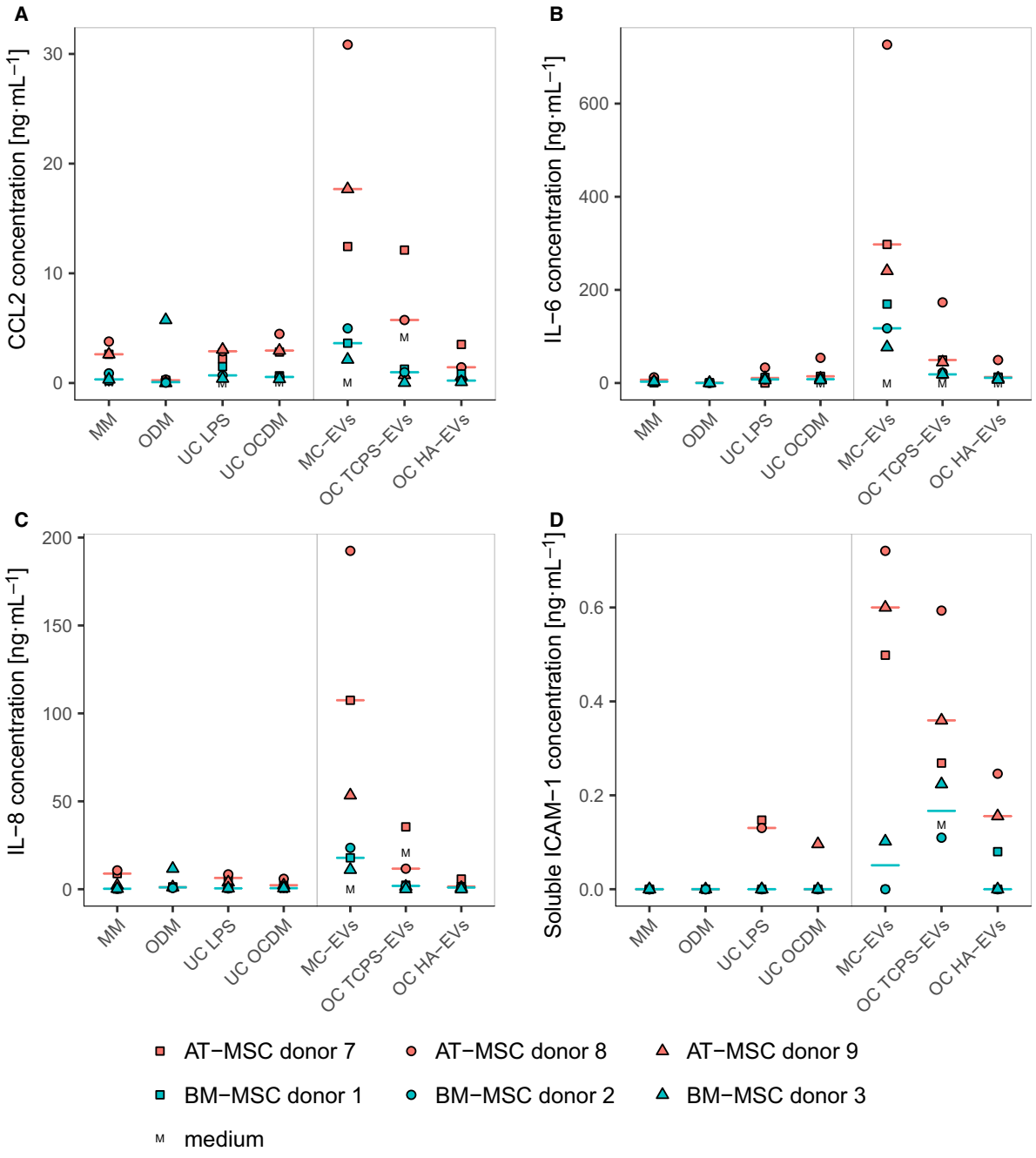

Fig. 13. Protein concentrations of CCL2 (A), IL-8 (B), IL-6 (C) and soluble ICAM-1 (D) measured using cytometric bead arrays in the AT-MSCs (pink fill) and BM-MSCs (blue fill). MSCs were cultured in EV-free MM, ODM or exposed to MC-EVs, OC TCPS-EVs or OC HA-EVs. MSCs were also cultured in MM supplemented with UC LPS or UC OCDM. Pink and blue bars indicate median expression for AT-MSCs and BM-MSCs, respectively. The protein concentration in the (supplemented) culture media before MSC culture are marked with the letter M.

isolated EVs were able to interact with target cells: AT-MSCs took up both MC-EVs and OC-EVs (Fig. 5). The same was previously found for BM-MSCs that took up EVs from LPS-activated MCs [20]) and dendritic cells [31], another mononuclear phagocytic cell type. These results suggest that many, if not all, mononuclear phagocytes interact with MSCs through their EVs. The EVs were found in clusters close to the nuclei, suggesting active endocytosis of the EVs leading to processing of their molecular cargo [31]. Other

mechanisms of interaction with the AT-MSCs cannot be ruled out, such as EV-mediated activation of membrane-bound receptors that trigger signalling pathways, or fusion with the cell membrane leading to release of the EV cargo into the cell cytoplasm [24].

Ekström *et al*. [20] found that uptake of MC-EVs by BM-MSCs differed largely between cells within the same culture and also between different experiments. Uptake of EVs could be affected by proliferation status and membrane composition [20]. Differences in uptake efficiency between the EVs of different origin were not the main interest of this study and would require a different experimental set-up. Conclusions EV-MSC interaction based on different numbers of DiD-labelled EVs inside the AT-MSCs (Fig. 5A–D) or on EV-positive AT-MSC fractions (Fig. 5E–G) should therefore be taken with care.

Isolated monocyte- and osteoclast-derived EVs carry different signals to MSCs

Current scientific literature is not unanimous about the effects of EVs derived from mononuclear phagocytes on MSCs. EV derived from LPS-activated MCs were reported to stimulate osteogenic differentiation of MSCs [20] and similar results have been reported for dendritic-cell derived EVs [32]. Silva *et al*. [31] on the other hand did not find any effects of dendritic-cell derived EVs on osteogenic differentiation, despite the accumulation of these EV inside the MSCs. Also the interactions between OCs, osteoblasts and mesenchymal precursors partially take place through tranfer of EVs. These interactions can also inhibit osteoblast activity, as OC-EVs are able to transfer miR-214-3p to inhibit osteoblast activity *in vitro* and reduce bone formation *in vivo* [33,34].

In the present study, we did not observe a significant effect of OC-EVs on gene expression in MSCs (Fig. 7). We chose to culture the AT-MSCs in equal numbers of MC- and OC-EVs in the microarray experiments, in order to compare their potency to change AT-MSC gene expression. When we analysed gene expression and protein secretion by AT-MSCs and BM-MSCs, we used EVs isolated from the same volume of conditioned medium so that they came from cultures with the same number of initially seeded MCs. OC-EVs did not have or had a smaller effect than MC-EVs, at least for the genes and proteins that we analysed (Figs 12 and 13). We cannot exclude that OC-EVs trigger signalling pathways different from the ones activated by MC-EVs, but that we would only detect if we had used more EVs. Characterizing the molecular cargo carried by MC-EVs and OC-EVs would provide insight in how the regulating potential of EVs changes when MCs differentiate into OCs.

Monocyte-derived EVs promote the secretion of various cytokines in MSCs, representing an immunomodulatory mechanism

Mesenchymal stem/stromal cells interact with the immune system by secreting anti-inflammatory factors, as well as by expressing cell surface molecules that suppress the maturation, activation and function of immune cells [35]. Their immunosuppressive properties make MSCs a relevant cell source when considering immunomodulation therapies and allogeneic stem cell treatments [36]. The immunosuppressive effects of MSCs are at least partially mediated by EVs [37]. Here, we show that MC-EVs upregulated the secretion of various cytokines by MSCs. Chemokine secretion by MSCs may represent an immunomodulatory mechanism in which chemotaxis brings specific immune cell subsets in close proximity to MSCs, which makes them more susceptible for the immunosuppressive actions of MSCs [38,39]. The response to MC-EVs was stronger in AT-MSCs than in BM-MSCs, reflecting the greater immunomodulatory potency of AT-MSCs [36].

Exposing MSCs to the UC precipitate of unconditioned LPS-supplemented medium (UC LPS and UC OCDM) did not affect gene expression nor protein secretion, except for *ICAM1* expression and the secretion of its protein product in AT-MSCs. We suspect that traces of LPS in the UC precipitate upregulated the expression of *ICAM1*. Upregulation of *ICAM1* in response to LPS has been long known in epithelial cells [40–42], but has so far not been reported in MSCs. LPS can suppress the osteogenic differentiation potential of MSCs through the Toll-like receptor 4 mediated nuclear factor κB pathway [43]. The differentiation potential of BM-MSCs, however, is not affected by LPS, showing that the response to LPS is dependent on the tissue source of the MSCs [43]. Likewise, in the present study, *ICAM1* expression in BM-MSCs was not affected by UC LPS and UC OCDM. Addition of EVs did not lead to differential expression of *ICAM1* compared to the aforementioned controls.

Monocyte-derived EVs upregulated expression of MMPs and might drive tissue remodelling processes

After OCs have finished resorbing a packet of bone, collagen fibrils are left in the resorption pit that protrude from the bone surface. The collagen fibrils need to be removed before new bone formation can take

place [44]. It has long been unknown which cells are responsible for the removal of these collagen fibrils. Given that mononuclear cells (lymphocytes and MCs) reside near the bone surface, it has been suggested that mononuclear phagocytes are involved in their removal [45]. Our data confirm that MCs might play a role by stimulating collagen removal through EV-mediated signalling. MC-EVs upregulated the expression of *MMP*s, thereby stimulating processes related to the reorganization of the extracellular matrix structure, in particular the removal of collagens. We show that *MMP*s are overexpressed in MSCs, suggesting that cells of mesencymal lineages start to remove collagens in response to the presence and activation of MCs. These results confirm the suggestion that bone lining cells clean the bone surface before new bone formation takes place [44]. Bone lining cells are mesenchymal cells and although bone lining cells do not form bone, they belong to the same lineage as osteoblasts. Although speculative, signals from MCs, combining both soluble factors and MC-EV interactions, may direct MSCs to differentiate towards bone lining cells.

Our results show the importance of EV-mediated signalling between MCs and MSCs for controlling the function of the immune system. The promotion of cytokine secretion by MC-EVs may enhance the immunosuppressive actions of the MSCs. EV-mediated signalling might represent an additional mode of intercellular communication during the transition from injury and inflammation to bone regeneration. The upregulation of *MMP*s suggests an important role of MC-EVs in the coupling between bone resorption and bone formation. Characterizing the molecular cargo carried by MC-EVs and OC-EVs would provide insight in how the regulating potential changes of the EVs when MCs differentiate into OCs.

Conclusion

Our results show the importance of EV-mediated signalling between MCs and MSCs for controlling the function of the immune system. MC-EVs promoted the secretion of various cytokines by MSCs. Chemokine secretion by MSCs may represent an immunomodulatory mechanism in which chemotaxis brings specific immune cell subsets in close proximity to MSCs, which makes them more susceptible for the immunosuppressive actions of MSCs. MC-EVs form promising prospects for the development of MSC-based immune therapy by enhancing the immunosuppressive actions of the MSCs.

Monocyte-EVs upregulated the expression of *MMPs*, thereby stimulating processes related to the reorganization of the extracellular matrix structure. Signals secreted by MCs may direct MSCs to differentiate towards bone lining cells. EV-mediated signalling might represent an additional mode of cell-cell signalling during the transition from injury and inflammation to bone regeneration and play an important role in the coupling between bone resorption and bone formation.

In the present study, we did not observe a significant effect of OC-EVs on gene expression in MSCs. We cannot exclude that OC-EVs trigger signalling pathways different from the ones activated by MC-EVs. Characterizing the molecular cargo carried by MC-EVs and OC-EVs would provide insight in how the regulating potential changes of the EVs when MCs differentiate into OCs.

Material and methods

Preparation of hydroxyapatite coatings in 24-well culture plates

Hydroxyapatite coatings were deposited in 24-well culture plates in a two-step procedure consisting of precalcification and crystal growth as described by Patntirapong *et al.* [18]. The 24-wells were precalcified using a 3 × concentrated simulated body fluid (SBF × 3) into each well. SBF × 3 was prepared by mixing calcium solution (820 mM NaCl, 8.9 mM $MgCl_2{\cdot}6H_2O$, 105 mM $CaCl_2{\cdot}2H_2O$) and phosphate solution (25 mM $NaHCO_3$, 1.9 mM $NaHPO_4{\cdot}2H_2O$), both of which were prepared in 50 mM Tris HCl buffer solution at pH 7.4. Freshly prepared SBF × 3 solution was added to each well (1.5 mL) and refreshed daily during a 3-day incubation period at room temperature. This resulted in the formation of a thin amorphous calcium phosphate coating that acted as nucleation layer for crystal growth in the second step. At the end of the precalcification, the wells were thoroughly washed in distilled H_2O and dried at 50 °C.

In the second step, calcium phosphate solution was prepared by dissolving 140 mM NaCl, 4 mM $CaCl_2{\cdot}2H_2O$ and 2.6 mM $NaHPO_4{\cdot}2H_2O$ in 50 mM Tris HCl buffer at pH 7.4. Calcium phosphate solution was added to the precalcified wells (1.5 mL) and refreshed daily during a 3-day incubation period at room temperature. The resulting HA coatings resemble the mineral component of bone. The HA coated wells were thoroughly washed in distilled H_2O and dried at 50 °C. Before use for cell cultures, the wells were sterilized by soaking in 70% ethanol and drying under ultraviolet light for 20 min.

Isolation of human monocytes

Human buffy coats were obtained from the Finnish Red Cross Blood Service (Helsinki, Finland). Buffy coats were left from the processing of blood collected from healthy

voluntary blood donors. Before blood donation, donors are informed that blood samples that are not required for patient treatment can be used anonymously for research work. The use of buffy coats for this project was approved by the ethical committee of the Finnish Red Cross Blood Service. The study methodologies conformed to the standards set by the Declaration of Helsinki.

Monocytes were isolated from 40 mL of buffy coat in a two-step procedure [46]. Briefly, peripheral blood mononuclear cells (PBMCs) were extracted from the buffy coats by gradient centrifugation. The buffy coat was diluted 1 : 1 with PBS and gently layered on top of Lymphoprep™ (StemCell Technologies, Vancouver, Canada). The gradient was centrifuged for 30 min at 800 ***g*** with the brake off. The PBMC layer was collected and washed several times with PBS.

Monocytes were isolated from the PBMC fraction by depletion of non-MCs (negative selection) using a MC Isolation kit II (Miltenyi Biotech, Bergisch Gladbach, Germany) according to the manufacturer's instructions. Briefly, non-MCs were indirectly magnetically labelled with a cocktail of biotin-conjugated monoclonal antibodies against CD3, CD7, CD16, CD19, CD56, CD123 and Glycophorin A. Anti-biotin monoclonal antibodies conjugated to microbeads were used to magnetically label non-MCs which were then retained in a magnetic field.

Culture of monocytes and generation of osteoclasts

Monocytes were plated at a density of 1.5×10^5 cells·cm^{-2} in 24-well plates, either on TCPS or coatings of HA. MCs were either activated by culturing in MM supplemented with 10 ng·mL^{-1} LPS (LPS-activation medium, Table 2) or stimulated to generate OCs in OCDM (Table 2). The cells were cultured at 37 °C and 5% CO_2 in a humidified atmosphere. The culture medium was refreshed every 2–3 days. LPS-activated MCs were cultured in EV-depleted medium from the start of the culture. The OC differentiation cultures were changed to EV-depleted OCDM once OCs had formed. EV-depleted OCDM was supplemented with LPS for the culture of cells from blood donors 3 and 4. EV-depleted medium was prepared with FBS depleted of EVs by UC for 19 h at 120 000 ***g*** (26 000 r.p.m. in an Optima LE-80K ultracentrifuge equipped with an SW-28 swinging-bucket rotor, Beckman Coulter, Inc., Brea, CA, USA).

At the beginning of the conditioned medium collection, samples were taken by fixing of the cells in 4% paraformaldehyde (Sigma-Aldrich, Saint Louis, MO, USA). To confirm the formation of OCs, the cells were stained for IC-specific marker TRAcP using the Leucocyte acid phosphatase kit (Sigma-Aldrich) according to the manufacturer's instructions. During the culture and after the staining, cells were monitored and imaged using a Nikon Eclipse TS100 inverted phase-contrast microscope (Nikon Corporation, Tokyo, Japan) equipped with a Nikon DS-Fi2 camera.

Table 2. The compositions of media used in the study

MM	DMEM/F-12 with GlutaMAX™ (Gibco®, Thermo Fisher Scientific), 10% FBS (Gibco®), 100 units·mL^{-1} penicillin and 100 μg·mL^{-1} streptomycin (Gibco®)
EV-depleted MM	DMEM/F-12 with GlutaMAX™, 10% EV-depleted FBS, 100 units·mL^{-1} penicillin and 100 μg·mL^{-1} streptomycin
LPS-activation medium	EV-depleted MM, 10 ng·mL^{-1} LPS (*Escherichiea coli* O111: B4, Merck Millipore, Billerica, MA, USA)
(EV-depleted) OCDM	(EV-depleted) MM, 10 ng·mL^{-1} recombinant human macrophage colony-stimulating factor (M-CSF, R&D systems), 20 ng·mL^{-1} RANK-L (Peprotech, Rocky Hill, NJ, USA), (10 ng·mL^{-1} LPS)
EV-depleted ODM	EV-depleted MM, 50 μM L-Ascorbic acid 2-phosphate (Sigma-Aldrich), 10 mM β-glycerophosphate disodium salt hydrate (Sigma-Aldrich), 100 nM dexamethasone (Sigma-Aldrich)

Collection of monocyte- and osteoclast-condition medium and isolation of extracellular vesicles

The conditioned medium was collected from the LPS-activated MCs at 3 and 5 days of culture. The conditioned medium from OCs was collected 3 days and 5 days after changing to EV-depleted medium. The conditioned medium was depleted of cell debris by centrifuging for 20 min at 2500 ***g*** and the supernatant was filtered through a 0.45 μm sterile filter (Merck, Darmstadt, Germany).

For blood donors 1 and 2, EVs were isolated from the conditioned medium using an isolation kit. The miRCURY™ Exosome Isolation Kit (Exiqon A/S, Vedbæk, Denmark) was used according to the manufacturer's instructions. Briefly, hydration of particles was diminished by mixing the media with the precipitation buffer provided in the kit. After incubation at 4 °C for minimally 1 h, the EVs were precipitated by centrifugation at 3000 ***g*** for 30 min. The supernatant was removed and the pellet was resuspended in the resuspension buffer provided in the kit. EVs were stored at −75 °C until further use.

For blood donor 3 and 4, EVs were isolated from the conditioned medium by UC for 2 h at 120 000 ***g***. The UC precipitate was washed by adding a large volume of filtered PBS (0.1 μm filter), after which UC was repeated. EVs were resuspended in filtered PBS and stored at −75 °C until further use.

Characterization of monocyte- and osteoclast-derived extracellular vesicles

Monocyte-EVs, OC TCPS-EVs or OC HA-EVs were characterized using transmisssion electron microscopy, nanoparticle tracking analysis and western blotting.

Extracellular vesicles were washed by diluting in PBS and ultracentrifuged for 2 h at 120 000 ***g***. The EV samples were resuspended in PBS and prepared for transmisssion electron microscopy as described previously [47]. After loading to 200 mesh copper grids and fixation with 2% paraformaldehyde in 0.1 M $NaPO_4$ buffer (pH 7.0), samples were washed with the 0.1 M $NaPO_4$ buffer and deionized water, negatively stained with 2% neutral uranyl acetate and embedded in methyl cellulose uranyl acetate mixture (1.8/0.4%). Samples were viewed with transmisssion electron microscopy using Tecnai 12 (FEI Company, Eindhoven, the Netherlands) operating at 80 kV. Images were taken with Gatan Orius SC 1000B CCD-camera (Gatan Inc., Pleasanton, CA, USA) with 4008 × 2672 px image size and no binning.

Nanoparticle tracking analysis was used to quantify and determine the size distribution of particles in the EV samples. EV samples were diluted in PBS and injected into the NanoSight LM14 (NanoSight Ltd., Salisbury, UK) equipped with a blue laser (405 nm, 60 mW) and a sCMOS camera. Three videos of 60 s (1498 frames each) were recorded and analysed using NANOSIGHT software v3.0 (Particular Sciences Ltd, Dublin, Ireland). Particles between 50 and 400 nm in diameter were considered EVs.

Western blotting was performed as described previously [47]. The following antibodies were used: mouse anti-Thy1 (CD90; Sigma-Aldrich, clone 3F9, 1 : 500), rabbit anti-TSG101 (Sigma-Aldrich, polyclonal, SKU HPA006161, 1 : 500), mouse anti-Hsp70 (BD Biosciences, Becton Dickinson, Franklin Lakes, NJ, USA, clone 5G10, 1 : 1000), mouse anti-CD63, (BD Biosciences, clone H5C6, 1 : 1000), mouse anti-CD14 (R&D systems, Minneapolis, MN, USA, clone 134603, 1 : 1000), mouse anti-RANK (receptor activator of nuclear factor the conditioned medium using an κ-B; Novus Biologicals, Littleton, CO, USA, clone 9A725, 1 : 1000) and rabbit anti-calnexin (Cell Signaling Technology, Leiden, the Netherlands, clone C5C9, 1 : 800). EVs were isolated by UC from equal volumes of conditioned medium and loaded to the gel. Protein from MC lysate was loaded to the gels as a control. EV samples were denatured at 95 °C for 5 min in reducing Laemmli sample buffer, separated using Mini-PROTEAN® TGX™ 4–20% gradient SDS/PAGE gels (Bio-Rad, Hercules, CA, USA) with page ruler prestained protein ladder (Thermo Fisher Scientific, Waltham, MA, USA) as a standard and blotted on Immobilon-P poly(vinylidene difluoride) membrane (Merck). Blocking and antibody incubations were performed in Odyssey blocking buffer (LI-COR BioSciences, Lincoln, NE, USA) without and with 0.1% Tween-20, respectively. Membranes were subsequently probed with IRDye® 800CW Goat anti-Mouse (LI-COR) at 1 : 15 000 for 2 h at room temperature. After incubation, membranes were washed three times in TBS-T for 10 min at room temperature and imaged on an Odyssey FC Imager (LI-COR). Anti-CD63 was applied to nonreduced samples.

We have submitted all relevant data of our EV experiments to the EV-TRACK knowledgebase (EV-TRACK ID: EV170018) [48].

Isolation and characterization of adipose tissue-derived and bone marrow-derived mesenchymal stem/stromal cells

The use of human MSCs confirmed to the standards set by the Declaration of Helsinki.

Human AT-MSCs were obtained from water-assisted lipotransfer liposuction aspirates [49] from nine female donors (median age 44.5, range: 32–60) using mechanical and enzymatic isolation as described previously [50]. The study was carried out under approval of the ethical committee of Helsinki and Uusimaa Hospital District and with informed consent from the donors.

Human BM-MSCs were isolated as described previously with slight modifications [51]. BM was obtained under approval of the ethical committee of the Pirkanmaa Hospital District (R15174) and the written consent of the patients. The BM was diluted 1 : 3 with Dulbecco's PBS (Gibco®; Thermo Fisher Scientific). The mixture was layered on a Histo Paque-1077 (Sigma-Aldrich) cushion and centrifuged at 800 ***g*** for 20 min at room temperature. Mononuclear cells were collected from the liquid interface and washed with αMEM (Lonza, Basel, Switzerland).

The MSCs were expanded in MM (Table 2) at 37 °C and 5% CO_2 in a humidified atmosphere.

After expansion, MSCs were characterized using a BD Accuri™ C6 flow cytometer (Becton Dickinson) to confirm the mesenchymal origin of the cells. We used monoclonal antibodies conjugated with allophycocyanin against CD14 (clone M5E2, 1 : 25), CD19 (clone HIB19, 1 : 25), CD34 (clone 581, 1 : 33), CD45RO (clone UCHL1, 1 : 33), CD54 (clone HA58, 1 : 33), CD73 (clone AD2, 1 : 143), CD90 (clone 5E10, 1 : 330), CD105 (clone 266, 1 : 100) and HLA-DR (clone G46-6, 1 : 25), all purchased from BD Pharmingen™ (Becton Dickinson). Analysis was performed on 1 × 10^5 events per sample and positive expression was defined as the level of fluorescence > 99% of the corresponding unstained cell sample.

Adipose tissue-MSCs and BM-MSCs demonstrated high expression of CD73 (ecto-5′-nucleotidase), CD90 (Thy-1) and CD105 (endoglin) and no or low expression of CD14 (MC and macrophage marker), CD19 (dendritic cell marker), CD45 (pan-leucocyte marker) and HLA-DR (human leucocyte antigen class II; Table 3). Moderate expression of CD34 (haemopoetic progenitor cell antigen) and CD54 (ICAM-1) in AT-MSC conforms to previous reports for culture in FBS [52]. The results showed that MSCs expressed most of the specific antigens that define human stem cells of mesenchymal origin according to the criteria set by the Mesenchymal and Tissue Stem Cell Committee of the ISCT [53].

Table 3. Surface marker expression by AT-MSCs and BM-MSCs used in this study. Cells were defined positive for a surface marker if the fluorescence level was > 99% of the corresponding unstained cell sample. CD, cluster of differentiation.

CD		Median positive expression (min–max)	
		AT-MSCs (n = 9)	BM-MSCs (n = 3)
CD14	LPS receptor, MC and macrophage marker	0.2% (0.0–0.5)	0.2% (0.2–0.4)
CD19	B-lymphocyte surface antigen B4	0.1% (0.0–0.2)	0.1% (0.1–0.2)
CD34	Protein tyrosine phosphatase receptor type C, leucocyte common antigen	13.0% (0.0–38.0)	0.2% (0.1–3.1)
CD45	Protein tyrosine phosphatase receptor type C, leucocyte common antigen	0.2% (0.0–0.7)	0.2% (0.2–0.3)
CD54	ICAM-1	60.8% (3.0–92.2)	13.3% (10.0–14.4)
CD73	ecto-5′-nucleotidase	100.0% (96.8–100.0)	99.4% (99.1–99.8)
CD90	Thy-1 T-cell surface glycoprotein	99.9% (96.0–100.0)	97.6% (97.6–97.6)
CD105	Endoglin, part of the TGF beta receptor complex	98.1% (92.0–99.8)	97.3% (95.2–97.4)
HLA-DR	Human leucocyte antigen – antigen D related	0.4% (0.1–1.2)	1.5% (0.8–1.6)

Uptake of monocyte- and osteoclast-derived EVs by adipose tissue-derived mesenchymal stem/stromal cells

Extracellular vesicles were labelled in 1 μM DiD lipophilic dye (Thermo Fisher Scientific) for 1 h at room temperature. The unbound dye was removed by adding a large volume of PBS and UC for 2 h at 120 000 ***g***. The washing step was performed twice before resuspending the EV pellet in EV-depleted MM. DiD-labelled PBS without EVs was processed the same way to serve as a control.

Adipose tissue-MSCs from donor 7 were seeded in 8-well chamber slides (Ibidi GmbH, Planegg, Germany) at passages 4 or 7 and 1×10^4 cells·cm^{-2}. The cells were allowed to attach in MM overnight before the medium was changed to EV-depleted MM supplemented with 3×10^9 DiD-labelled EVs·mL^{-1} based on nanoparticle tracking analysis (1.5×10^5 EVs per cell), or to EV-depleted MM supplemented with the PBS control. After 3 days, the cells were labelled with 5 μM CellTrace™ CFSE dye (Thermo Fisher Scientific) and 1 μg·mL^{-1} Hoechst 33342 (Sigma-Aldrich), both for 20 min at 37 °C. The cells were washed prior to imaging. Microscopy was performed on a TCS CARS SP8 confocal microscope (Leica Microsystems GmbH, Wetzlar, Germany) with a 63× water immersion objective.

After imaging, cells were detached by trypsin treatment and analysed by flow cytometry (BD Accuri® C6). DiD fluorescence intensity was detected using the FL4 channel (675/25 nm laser). The data were analysed and visualized using R Statistical Software (R Foundation for Statistical Computing, Vienna, Austria).

Exposure of adipose tissue-derived and bone marrow-derived mesenchymal stem/stromal cells to monocyte- and osteoclast-derived EVs

Adipose tissue-MSCs and BM-MSCs were seeded in 96-well plates at passages 4–6 and 2.5×10^3 cells·cm^{-2}. The cells were allowed to attach in MM overnight before the medium was changed to EV-depleted MM supplemented with 3×10^9 EVs·mL^{-1} based on nanoparticle tracking analysis (6×10^5 EVs per cell). Cells cultured in EV-depleted MM and cells cultured in EV-depleted ODM (Table 2) were used as controls. In addition, we supplementing the MSC culture medium with UC precipitate from LPS-activation medium (UC LPS) and LPS-supplemented OCDM (UC OCDM) that had not been in with cells, to control for the effect of particles from the culture media coprecipitated with the EVs.

The cells were cultured at 37 °C and 5% CO_2 in a humidified atmosphere for 18 days or 19 days, during which the medium was refreshed every 2–3 days. Each time, EVs were freshly added. At the end of the culture, the wells were washed in PBS and the contents were collected for analysis. For analysis of protein secretion, the MSC-conditioned medium was collected, depleted of cell debris by centrifuging for 20 min at 2500 ***g*** and stored at −75 °C until further use.

Gene expression analyses by microarrays and quantitative PCR

Total RNA was isolated from MSCs using the miRCURY™ RNA Isolation Kit (Exiqon A/S) according to the manufacturer's instructions. Concentration and purity of RNA was measured with the Agilent 2200 TapeStation (Agilent Technologies, Foster City, CA, USA) or NanoDrop-1000 (Thermo Fisher Scientific).

For the microarray analysis, the RNA from 5 AT-MSC donors (donor 1–5) was pooled into three distinct pools per condition. The starting amount of total RNA was 100 ng. cDNA was generated using GeneChip® WT Plus Reagent Kit (Affymetrix, Inc., Santa Clara, CA, USA). Micorarray analysis was performed using Clariom D Human Arrays (Affymetrix), which contain 135 750 human gene probes. Moderated paired t-tests were performed using the limma package in R based on Bayesian statistics and fitting of data to a linear model [54]. A false discovery rate of < 0.05 was used to filter differentially expressed genes between treatments and control (EV-depleted MM). A heat map was generated using the expression values of differentially

expressed genes transformed to *Z*-scores and subsequent hierarchical clustering based on Euclidean distances.

The microarray data discussed in this publication have been deposited in NCBI's Gene Expression Omnibus [55] and are accessible through GEO Series accession number GSE102401.

Functional enrichment was assessed by enrichment analysis of gene ontology terms for genes differentially expressed in the presence of MC-EVs compared to control (EV-depleted MM). GOSTATS package (v3.5) for R was used to compute the hypergeometric test and detect significantly over-represented biological processes and molecular functions affected by changes in the transcriptome [56]. Each list of differentially expressed transcripts was tested against the total list of transcripts in our analysis after filtering out transcripts without Entrez Gene ID or gene ontology annotation.

Gene expression was analysed using qPCR. Total RNA was converted into cDNA by reverse transcription using a High-Capacity cDNA Reverse Transcription Kit (Thermo Fisher Scientific). The expression of specific genes was quantified using TaqMan® assays (Thermo Fisher Scientific) for the following genes: aggrecan (*ACAN*, assay ID Hs00153936_m1), alkaline phosphatase, liver/bone/kidney (*ALPL*, assay ID Hs01029144_m1), bone morphogenetic protein 2 (*BMP2*, assay ID Hs00154192_m1), collagen type XV alpha 1 chain (*COL15A1*, assay ID Hs00266332_m1), C–X–C motif chemokine 5 (*CXCL5*, assay ID Hs00171085_m1), fibrinogen like 2 (*FGL2*, assay ID Hs00173847_m1), *ICAM1* (assay ID Hs00164932_m1), integrin subunit alpha 3 (*ITGA3*, assay ID Hs01076879_m1), matrix metallopeptidase 1 (*MMP1*, assay ID Hs00899658_m1) and runt-related transcription factor 2 (*RUNX2*, assay ID Hs01047973_m1). Genes were selected based on their established relevance to osteogenesis, or based on their differential expression in the presence of EVs compared to EV-depleted MM in our array data. The PCR reactions were conducted in triplicates in an Applied Biosystems® 7500 Fast Real-Time PCR System (Thermo Fisher Scientific). The results were adjusted for the efficiency of the chain reactions according to the method described by Yuan *et al.* [57] and normalized to the geometrical average of multiple reference genes: ribosomal protein lateral stalk subunit P0 (*RPLP0*, assay ID Hs99999902_m1), TATA-binding protein (*TBP*, assay ID Hs00427620_m1) and *YWHAZ* (tyrosine 3-monooxygenase/tryptophan 5-monooxygenase activation protein zeta, assay ID Hs03044281_g1), which have been shown to be stably expressed under several experimental conditions [58].

Biochemical analyses

Adipose tissue-MSCs (donors 1–6) were lysed in 0.1% triton-x-100 (Sigma-Aldrich) and frozen at −75 °C. Alkaline phosphate activity was measured by mixing the cell lysate with *p*-nitrophenyl phosphate (Sigma-Aldrich) and 2-amino-2-methyl-1-propanol (Sigma-Aldrich). The amount of produced *p*-nitrophenol was measured in a Victor™ X4 multiplate reader (PerkinElmer Inc., Waltham, MA, USA) at 405 nm.

Total collagen content was quantified using a hydroxyproline assay (Sigma-Aldrich). Hydroxyproline content is a good measure of total collagen content, assuming that elastin content is negligible [59]. The cell lysate was hydrolysed in 6 N hydrochloric acid (Sigma-Aldrich) at 110 °C for 3 h followed by quantification of hydroxyproline content based on the reaction of oxidized hydroxyproline with 4-(dimethylamino)benzaldehyde. Absorbance was measured at 544 nm in the multiplate reader.

To normalize the alkaline phosphate activity and total collagen content for cell number, the amount of DNA in the cell culture lysates was quantified using 0.2 $\mu g \cdot mL^{-1}$ Hoechst 33258 nucleic acid stain (Bio-Rad Laboratories Inc.) with purified calf thymus DNA as a standard (Bio-Rad). Fluorescence was measured with the multiplate reader using excitation at 360 nm and emission at 460 nm.

Cytometric bead arrays for quantification of protein secretion

The concentration of ILs and chemokines in the AT-MSC-(donors 7–9) and BM-MSC-conditioned media were analysed using cytometric bead arrays according to the manufacturer's instruction on a BD Accuri C6 flow cytometer. In addition, we analysed the unconditioned (EV-supplemented) media to check for proteins present in the media without the MSCs. We employed a human chemokine kit with specific antibodies for IL-8, CCL5, CXCL9, CCL2, and CXCL10 (BD Biosciences, cat. no. 552990) and a flex set array for IL-6 (BD Biosciences, cat. no. 558276) on 1 : 100 diluted conditioned media. Undiluted media were analysed with a flex set array for soluble ICAM-1 (BD Biosciences, cat. no. 560269). CBA output data were analysed using FCAP ARRAY software version 3.0 (BD Biosciences).

Statistical analyses

Statistical analyses were performed with R Statistical Software. The effects of medium composition and EV source on alkaline phosphatase activity, total collagen content (Fig. 11) and gene expression levels (Fig. 8) in AT-MSC cultures were analysed using Kruskal–Wallis one-way analysis of variance by ranks. Mann–Whitney *U post hoc* tests were conducted to analyse specific conditions against the control (EV-depleted MM) for significant differences. Paired *t*-tests were performed to test for statistically significant differences in gene expression (Fig. 12) and secreted protein levels (Fig. 13) between MSCs exposed to MC-EVs and UC LPS, between OC-EVs and UC OCDM, as well as ODM, UC LSPS and UC OCDM against MM. The results

were considered significant when the false discovery rate-controlled *P*-value was below 0.05.

Acknowledgements

The authors thank the Biomedicum Flow Cytometry Core Facility, the EV Core Facility, the Electron Microscopy Unit of the Institute of Biotechnology, the Biomedicum Functional Genomics Unit (FUGU) and the Biomedicum Imaging Unit, University of Helsinki for providing laboratory facilities and services. We thank Yusuf Khan, MSc for his expert advice on the microarray analysis and Heidi Husu for her excellent technical assistance. This research was supported by University of Helsinki project funding (WBS490302, WBS73714112), the Jouko Pentikäinen fund from the Finnish Cultural Foundation, Helsinki University Hospital State funding for university-level health research (Y1014SUL05, TYH2016130), the EU's Erasmus+ staff mobility program and the Chancellor's travel grant for doctoral candidates in the Doctoral Program in Oral Sciences (FINDOS Helsinki).

Author contributions

AG planned and performed experiments, analysed and interpreted the data and wrote the manuscript. SK planned experiments and proofread the manuscript. RK collected and assembled data and proofread the manuscript. SM and HP provided study material. SH supported in administration. BM planned the experiments, supported in administration and proofread the manuscript. RSK supported in administration and proofread the manuscript.

References

1 Ratajczak J, Wysoczynski M, Hayek F, Janowska-Wieczorek A & Ratajczak MZ (2006) Membrane-derived microvesicles: important and underappreciated mediators of cell-to-cell communication. *Leukemia* **20**, 1487–1495.

2 Valadi H, Ekström K, Bossios A, Sjöstrand M, Lee JJ & Lötvall JO (2007) Exosome-mediated transfer of mRNAs and microRNAs is a novel mechanism of genetic exchange between cells. *Nat Cell Biol* **9**, 654–659.

3 Sims NA & Martin TJ (2014) Coupling the activities of bone formation and resorption: a multitude of signals within the basic multicellular unit. *Bonekey Rep* **3**, 481.

4 Liu M, Sun Y & Zhang Q (2018) Emerging role of extracellular vesicles in bone remodeling. *J Dent Res*. https://doi.org/10.1177/0022034518764411

5 Xie Y, Chen Y, Zhang L, Ge W & Tang P (2017) The roles of bone-derived exosomes and exosomal microRNAs in regulating bone remodelling. *J Cell Mol Med* **21**, 1033–1041.

6 de Jong OG, van Balkom BW, Schiffelers RM, Bouten CV & Verhaar MC (2014) Extracellular vesicles: potential roles in regenerative medicine. *Front Immunol* **5**, 608.

7 Narayanan R, Huang CC & Ravindran S (2016) Hijacking the cellular mail: exosome mediated differentiation of mesenchymal stem cells. *Stem Cells Int* **2016**, 3808674.

8 Qin Y, Sun R, Wu C, Wang L & Zhang C (2016) Exosome: a novel approach to stimulate bone regeneration through regulation of osteogenesis and angiogenesis. *Int J Mol Sci* **17**, 712.

9 Julier Z, Park AJ, Briquez PS & Martino MM (2017) Promoting tissue regeneration by modulating the immune system. *Acta Biomater* **53**, 13–28.

10 Dong L & Wang C (2013) Harnessing the power of macrophages/monocytes for enhanced bone tissue engineering. *Trends Biotechnol* **31**, 342–346.

11 Hume DA (2006) The mononuclear phagocyte system. *Curr Opin Immunol* **18**, 49–53.

12 Pirraco RP, Reis RL & Marques AP (2013) Effect of monocytes/macrophages on the early osteogenic differentiation of hBMSCs. *J Tissue Eng Regen Med* **7**, 392–400.

13 Champagne CM, Takebe J, Offenbacher S & Cooper LF (2002) Macrophage cell lines produce osteoinductive signals that include bone morphogenetic protein-2. *Bone* **30**, 26–31.

14 Boyce BF (2013) Advances in the regulation of osteoclasts and osteoclast functions. *J Dent Res* **92**, 860–867.

15 Pederson L, Ruan M, Westendorf JJ, Khosla S & Oursler MJ (2008) Regulation of bone formation by osteoclasts involves Wnt/BMP signaling and the chemokine sphingosine-1-phosphate. *Proc Natl Acad Sci USA* **105**, 20764–20769.

16 Henriksen K, Andreassen KV, Thudium CS, Gudmann KN, Moscatelli I, Cruger-Hansen CE, Moscatelli I, Crüger-Hansen CE, Schulz AS, Dziegiel MH *et al.* (2012) A specific subtype of osteoclasts secretes factors inducing nodule formation by osteoblasts. *Bone* **51**, 353–361.

17 Silva AM, Teixeira JH, Almeida MI, Gonçalves RM, Barbosa MA & Santos SG (2017) Extracellular vesicles: immunomodulatory messengers in the context of tissue repair/regeneration. *Eur J Pharm Sci* **98**, 86–95.

18 Patntirapong S, Habibovic P & Hauschka PV (2009) Effects of soluble cobalt and cobalt incorporated into calcium phosphate layers on osteoclast differentiation and activation. *Biomaterials* **30**, 548–555.

19 ten Harkel B, Schoenmaker T, Picavet DI, Davison NL, de Vries TJ & Everts V (2015) The foreign body giant cell cannot resorb bone, but dissolves hydroxyapatite like osteoclasts. *PLoS ONE* **10**, e0139564.
20 Ekström K, Omar O, Graneli C, Wang X, Vazirisani F & Thomsen P (2013) Monocyte exosomes stimulate the osteogenic gene expression of mesenchymal stem cells. *PLoS ONE* **8**, e75227.
21 Wright SD, Ramos RA, Tobias PS, Ulevitch RJ & Mathison JC (1990) CD14, a receptor for complexes of lipopolysaccharide (LPS) and LPS binding protein. *Science* **249**, 1431–1433.
22 Omar OM, Graneli C, Ekström K, Karlsson C, Johansson A, Lausmaa J, Wexell CL & Thomsen P (2011) The stimulation of an osteogenic response by classical monocyte activation. *Biomaterials* **32**, 8190–8204.
23 Sunkara V, Woo HK & Cho YK (2016) Emerging techniques in the isolation and characterization of extracellular vesicles and their roles in cancer diagnostics and prognostics. *Analyst* **141**, 371–381.
24 Raposo G & Stoorvogel W (2013) Extracellular vesicles: exosomes, microvesicles, and friends. *J Cell Biol* **200**, 373–383.
25 Lötvall J, Hill AF, Hochberg F, Buzás EI, Di Vizio D, Gardiner C, Gho YS, Kurochkin IV, Mathivanan S, Quesenberry P *et al.* (2014) Minimal experimental requirements for definition of extracellular vesicles and their functions: a position statement from the International Society for Extracellular Vesicles. *J Extracell Vesicles* **3**, 26913.
26 Booth AM, Fang Y, Fallon JK, Yang JM, Hildreth JE & Gould SJ (2006) Exosomes and HIV Gag bud from endosome-like domains of the T cell plasma membrane. *J Cell Biol* **172**, 923–935.
27 Théry C, Ostrowski M & Segura E (2009) Membrane vesicles as conveyors of immune responses. *Nat Rev Immunol* **9**, 581–593.
28 Edelman DA, Jiang Y, Tyburski JG, Wilson RF & Steffes CP (2007) Lipopolysaccharide up-regulates heat shock protein expression in rat lung pericytes. *J Surg Res* **140**, 171–176.
29 Willms E, Johansson HJ, Mäger I, Lee Y, Blomberg KE, Sadik M, Alaarg A, Smith CI, Lehtiö J, El Andaloussi S *et al.* (2016) Cells release subpopulations of exosomes with distinct molecular and biological properties. *Sci Rep* **6**, 22519.
30 Huynh N, VonMoss L, Smith D, Rahman I, Felemban MF, Zuo J, Rody WJ Jr, McHugh KP & Holliday LS (2016) Characterization of regulatory extracellular vesicles from osteoclasts. *J Dent Res* **95**, 673–679.
31 Silva AM, Almeida MI, Teixeira JH, Maia AF, Calin GA, Barbosa MA & Santos SG (2017) Dendritic cellderived extracellular vesicles mediate mesenchymal stem/stromal cell recruitment. *Sci Rep* **7**, 1667.
32 Wang Z, Ding L, Zheng XL & Wang HX, Yan HM (2014) [DC-derived exosomes induce osteogenic differentiation of mesenchymal stem cells]. *Zhongguo Shi Yan Xue Ye Xue Za Zhi* **22**, 600–604.
33 Li D, Liu J, Guo B, Liang C, Dang L, Lu C, He X, Cheung HY, Xu L, Lu C *et al.* (2016) Osteoclast-derived exosomal miR-214-3p inhibits osteoblastic bone formation. *Nat Commun* **7**, 10872.
34 Sun W, Zhao C, Li Y, Wang L, Nie G, Peng J, Wang A, Zhang P, Tian W, Li Q *et al.* (2016) Osteoclast-derived microRNA-containing exosomes selectively inhibit osteoblast activity. *Cell Discov* **2**, 16015.
35 Hoogduijn MJ (2015) Are mesenchymal stromal cells immune cells? *Arthritis Res Ther* **17**, 88.
36 Mattar P & Bieback K (2015) Comparing the immunomodulatory properties of bone marrow, adipose tissue, and birth-associated tissue mesenchymal stromal cells. *Front Immunol* **6**, 560.
37 Fierabracci A, Del Fattore A, Luciano R, Muraca M, Teti A & Muraca M (2015) Recent advances in mesenchymal stem cell immunomodulation: the role of microvesicles. *Cell Transplant* **24**, 133–149.
38 Hoogduijn MJ, Popp F, Verbeek R, Masoodi M, Nicolaou A, Baan C & Dahlke MH (2010) The immunomodulatory properties of mesenchymal stem cells and their use for immunotherapy. *Int Immunopharmacol* **10**, 1496–1500.
39 Quaedackers ME, Baan CC, Weimar W & Hoogduijn MJ (2009) Cell contact interaction between adiposederived stromal cells and allo-activated T lymphocytes. *Eur J Immunol* **39**, 3436–3446.
40 Lee CH, Reid YA, Jong JS & Kang YH (1995) Lipopolysaccharide-induced differential cell surface expression of intercellular adhesion molecule-1 in cultured human umbilical cord vein endothelial cells. *Shock* **3**, 96–101.
41 Fakler CR, Wu B, McMicken HW, Geske RS & Welty SE (2000) Molecular mechanisms of lipopolysaccharide induced ICAM-1 expression in A549 cells. *Inflamm Res* **49**, 63–72.
42 Madjdpour C, Oertli B, Ziegler U, Bonvini JM, Pasch T & Beck-Schimmer B (2000) Lipopolysaccharide induces functional ICAM-1 expression in rat alveolar epithelial cells *in vitro*. *Am J Physiol Lung Cell Mol Physiol* **278**, L572–L579.
43 Li C, Li B, Dong Z, Gao L, He X, Liao L, Hu C, Wang Q & Jin Y (2014) Lipopolysaccharide differentially affects the osteogenic differentiation of periodontal ligament stem cells and bone marrow mesenchymal stem cells through Toll-like receptor 4 mediated nuclear factor κB pathway. *Stem Cell Res Ther* **5**, 67.
44 Everts V, Delaisse JM, Korper W, Jansen DC, Tigchelaar-Gutter W, Saftig P & Beertsen W (2002) The bone lining cell: its role in cleaning Howship's

lacunae and initiating bone formation. *J Bone Miner Res* **17**, 77–90.
45 Van Tran P, Vignery A & Baron R (1982) An electron-microscopic study of the bone-remodeling sequence in the rat. *Cell Tissue Res* **225**, 283–292.
46 Hafsi N, Voland P, Schwendy S, Rad R, Reindl W, Gerhard M & Prinz C (2004) Human dendritic cells respond to Helicobacter pylori, promoting NK cell and Th1-effector responses *in vitro*. *J Immunol* **173**, 1249–1257.
47 Puhka M, Nordberg ME, Valkonen S, Rannikko A, Kallioniemi O, Siljander P & Af Hällström TM (2017) KeepEX, a simple dilution protocol for improving extracellular vesicle yields from urine. *Eur J Pharm Sci* **98**, 30–39.
48 EV-TRACK Consortium, van Deun J, Mestdagh P, Agostinis P, Akay Ö, Anand S, Anckaert J, Martinez ZA, Baetens T, Beghein E *et al.* (2017) EV-TRACK: transparent reporting and centralizing knowledge in extracellular vesicle research. *Nat Methods* **4**, 228–232.
49 Peltoniemi HH, Salmi A, Miettinen S, Mannerstrom B, Saariniemi K, Mikkonen R, Kuokkanen H & Herold C (2013) Stem cell enrichment does not warrant a higher graft survival in lipofilling of the breast: a prospective comparative study. *J Plast Reconstr Aesthet Surg* **66**, 1494–1503.
50 Mesimäki K, Lindroos B, Törnwall J, Mauno J, Lindqvist C, Kontio R, Miettinen S & Suuronen R (2009) Novel maxillary reconstruction with ectopic bone formation by GMP adipose stem cells. *Int J Oral Maxillofac Surg* **38**, 201–209.
51 Li Z, Kupcsik L, Yao SJ, Alini M & Stoddart MJ (2009) Chondrogenesis of human bone marrow mesenchymal stem cells in fibrin-polyurethane composites. *Tissue Eng Part A* **15**, 1729–1737.
52 Patrikoski M, Juntunen M, Boucher S, Campbell A, Vemuri MC, Mannerström B & Miettinen S (2013) Development of fully defined xeno-free culture system for the preparation and propagation of cell therapy-compliant human adipose stem cells. *Stem Cell Res Ther* **4**, 27.
53 Dominici M, Le Blanc K, Mueller I, Slaper-Cortenbach I, Marini F, Krause D, Prockop DJ & Horwitz E (2006) Minimal criteria for defining multipotent mesenchymal stromal cells. The International Society for Cellular Therapy position statement. *Cytotherapy* **8**, 315–317.
54 Ritchie ME, Phipson B, Wu D, Hu Y, Law CW, Shi W & Smyth GK (2015) limma powers differential expression analyses for RNA-sequencing and microarray studies. *Nucleic Acids Res* **43**, e47.
55 Edgar R, Domrachev M & Lash AE (2002) Gene expression omnibus: NCBI gene expression and hybridization array data repository. *Nucleic Acids Res* **30**, 207–210.
56 Falcon S & Gentleman R (2007) Using GOstats to test gene lists for GO term association. *Bioinformatics* **23**, 257–258.
57 Yuan JS, Wang D & Stewart CN (2008) Statistical methods for efficiency adjusted real-time PCR quantifcation. *Biotechnol J* **3**, 112–123.
58 Ragni E, Vigano M, Rebulla P, Giordano R & Lazzari L (2013) What is beyond a qRT-PCR study on mesenchymal stem cell differentiation properties: how to choose the most reliable housekeeping genes. *J Cell Mol Med* **17**, 168–180.
59 Edwards CA & O'Brien WD (1980) Modified assay for determination of hydroxyproline in a tissue hydrolyzate. *Clin Chim Acta* **104**, 161–167.